



UNIVERSITY OF LEEDS

This is a repository copy of *Development of texturized legume protein from peas (Pisum sativum L.) and shiitake mushroom (Lentinus edodes P.): optimization and characterization approach*.

White Rose Research Online URL for this paper:

<https://eprints.whiterose.ac.uk/id/eprint/227114/>

Version: Accepted Version

Article:

Hisham, N.A.N., Yusoff, A., Seow, E.K. et al. (2 more authors) (2025) Development of texturized legume protein from peas (*Pisum sativum* L.) and shiitake mushroom (*Lentinus edodes* P.): optimization and characterization approach. *European Food Research and Technology*. ISSN 1438-2377

<https://doi.org/10.1007/s00217-025-04762-6>

This is an author produced version of an article published in *European Food Research and Technology*, made available under the terms of the Creative Commons Attribution License (CC-BY), which permits unrestricted use, distribution and reproduction in any medium, provided the original work is properly cited.

Reuse

This article is distributed under the terms of the Creative Commons Attribution (CC BY) licence. This licence allows you to distribute, remix, tweak, and build upon the work, even commercially, as long as you credit the authors for the original work. More information and the full terms of the licence here:

<https://creativecommons.org/licenses/>

Takedown

If you consider content in White Rose Research Online to be in breach of UK law, please notify us by emailing eprints@whiterose.ac.uk including the URL of the record and the reason for the withdrawal request.



eprints@whiterose.ac.uk
<https://eprints.whiterose.ac.uk/>

DEVELOPMENT OF TEXTURIZED LEGUME PROTEIN FROM PEAS (*Pisum sativum* L.) AND SHIITAKE MUSHROOM (*Lentinus edodes* P.): OPTIMIZATION AND CHARACTERIZATION APPROACH

Nur Annisa Noor Hisham¹, Anida Yusoff^{1,2*}, Eng Keng Seow^{1,2}, Brent S. Murray³, Alan Javier Hernandez Alvarez³

¹ Department of Food Science and Technology, Faculty of Applied Sciences, Universiti Teknologi MARA, Shah Alam 40450, Selangor, Malaysia; 2022142175@student.uitm.edu.my (N.A.N.H.); ekseow@uitm.edu.my (S.E.K.)

² Food Science Research Group, Faculty of Applied Sciences, Universiti Teknologi MARA, Shah Alam 40450, Selangor, Malaysia

³ School of Food Science and Nutrition, Faculty of Environment, University of Leeds, Leeds, United Kingdom; B.S.Murray@food.leeds.ac.uk (B.S.M.); A.J.HernandezAlvarez@leeds.ac.uk (A.J.H.A.)

***Corresponding author:** Anida Yusoff. Tel: +60 3-55447854, Email: anida@uitm.edu.my, Postal Address: Department of Food Science and Technology, Faculty of Applied Sciences, Universiti Teknologi MARA, 40450 Shah Alam, Selangor, Malaysia

ABSTRACT

The development of texturized legume proteins (TLP), especially from pea proteins is influenced by the globular nature of plant proteins, which can hinder the formation of fibrous structures. This study demonstrated that optimised extrusion conditions effectively enhanced the fibrous structure of texturized pea-shiitake mushroom (TPSM) protein using a single-screw extrusion process. A Box-Behnken design under response surface methodology was applied to optimise feed mixtures composition (pea protein isolate (PPI) and shiitake mushroom (SM)), barrel temperature, and screw speed. The optimal conditions identified were 80.91% PPI, 19.09% SM, a barrel temperature of 150°C, and a screw speed of 151.41 rpm. These conditions significantly influenced the integrity index (II) and water absorption capacity (WAC), with barrel temperature being the most influential factor. Increasing barrel temperature improved both II and WAC, contributing to enhanced texturization. Chemical analysis revealed a protein content of 73.49±0.3% in TPSM, with a favourable amino acid profile following extrusion. Protein solubility decreased significantly after extrusion. Functional analysis showed a significantly higher WAC, a significantly lower oil absorption capacity, no gelling formation at concentration 2-20% (w/v), and no significant effects on foaming and emulsification properties. These findings provide insights into optimising plant-based protein texturization for improved functionality in alternative protein applications.

Keywords: Texturization; Legume protein; Shiitake mushroom; Functional properties; Pea protein; Extrusion process optimisation

1. Introduction

Proteins are vital macronutrients essential for human growth and tissue maintenance [1]. The recommended daily intake for adults' ranges from 0.8-1.52 g/kg, with a minimum intake of 0.66 g/kg necessary to prevent deficiencies [2,3]. However, ensuring adequate protein intake remains a global challenge, particularly in developing regions, where access to protein-rich foods is often limited due to the high cost of animal-based proteins, health concerns, environmental sustainability issues, and ethical considerations [4,5]. The nutritional quality of proteins is typically evaluated based on their essential amino acid composition and digestibility. Animal proteins are considered complete due to their balanced amino acid profiles, whereas plant proteins often lack one or more of these essential components [3,6]. These factors contribute to dietary insufficiencies, raising concerns about food security and malnutrition. In response, there is growing global interest in plant-based proteins as a sustainable, cost-effective, and nutritionally viable alternative to help meet protein demands and enhance food security [7].

Textured vegetable protein (TVP), also referred to as textured legume protein (TLP) when derived from legume, is widely used as a meat analogue due to its fibrous structure and versatility in food applications [8]. Traditionally, TVP has been produced from soy protein, given its functional properties and high protein content. However, with growing demand for diverse protein alternatives sources, attention has shifted towards other legume proteins, such as pea protein isolate (PPI), which offers a high protein content (80–87%) and a balanced amino acid profile [6-7,9,10]. Peas (*Pisum sativum* L.), also provide additional health benefits due to their rich composition of complex carbohydrates, vitamins, and minerals, which contribute to cholesterol reduction, blood sugar regulation, and improved digestive health [11,12]. Despite these advantages, PPI is deficient in sulfur-containing amino acids (methionine and cysteine), which may limit its overall protein quality in comparison to soy protein [5]. Nevertheless, studies have shown that pea protein and its isolates meet the essential amino acid requirements established by the FAO/WHO/UNU [3]. Through appropriate extrusion processing, peas can serve as a valuable raw material for producing TLP via extrusion, offering a cost-effective protein source for vegetarian consumers [13].

Extrusion technology is a widely used high-temperature, short-time (HTST) process for transforming plant proteins into structured, fibrous products resembling meat [13,15]. This process combines heat, pressure, and mechanical forces, which induce complex transformations in protein structures. During extrusion, proteins undergo denaturation, unfolding, and molecular rearrangement, facilitating the formation of a three-dimensional fibrous network that mimics meat texture. The application of shear forces within the extruder further promotes protein alignment, contributing to the development of this fibrous structure. The disruption of non-covalent interactions, including hydrogen bonds and hydrophobic interactions, alongside the formation of new disulfide bonds, plays a crucial role in stabilising this network [15-17]. These structural changes significantly influence protein chemical and functional properties, such as solubility, water and oil absorption, gelling capacity, as well as emulsion and foaming properties [18,19]. Despite these mechanisms, achieving a well-defined fibrous texture with legume-based proteins, like pea protein, remains challenging due to their predominantly globular structure, which hinders the formation of stable network during extrusion [17,20]. The interplay between protein type, extrusion parameter, and additional ingredients is crucial in enhancing texture and improving the overall quality of TLP [10,20,21]. Consequently, the incorporation of supplementary ingredients has become essential to strengthen protein interactions and improve the fibrous structure of TLP. Edible mushrooms, such as shiitake mushrooms (*Lentinula edodes* P., SM), offer a promising option due to their high protein content, rich umami flavor, and functional components that contribute to improved texture and binding properties in food formulations [3,10,22].

SM, a widely consumed edible mushroom from the order Agaricales and family Omphalotaceae, is nutrient dense. It contains approximately 90% moisture, 67.5 % carbohydrates, 17.5% protein, and 8% fat and ash. SM is rich in essential amino acids, unsaturated fatty acids, and bioactive compounds such as amino-based molecules, peptide chains, glycoproteins, phenolic compounds, terpenoid structures, and carbohydrate-binding proteins. They also serve as a natural source of vitamin D and B-complex vitamins, providing additional health benefits beyond

their role in protein enhancement [19,22-24]. In traditional Asian medicine, SM have been associated with various therapeutic properties, including immune modulation, cholesterol reduction, and potential anticancer effects [19,22-24]. Their incorporation into extruded protein products has been explored to enhance nutritional quality and functionality; however, the impact of shiitake mushroom inclusion on the textural and functional properties of PPI-based TLP remains underexplored [4].

Extrusion conditions, including feed composition, barrel temperature, and screw speed, significantly influence the final structural and functional properties of TLP [18,25]. While some properties, such as water retention and texture, can be improved, others, such as solubility and gelling capacity, may be negatively affected depending on processing conditions [17,20]. Optimising these parameters is essential for producing high-quality TLP with desirable physicochemical properties [18,25]. Despite extensive research on TLP production from soy and other legumes, limited studies have examined the optimal formulation of PPI blended with SM to enhance texture, functionality, and overall product quality [4].

Response surface methodology (RSM) is widely used to optimise extrusion conditions, allowing for precise control over multiple processing variables [13]. This study employs a Box-Behnken Design (BBD) in RSM to achieve two key objectives: (1) to optimise extrusion process factors, including feed mixtures (PPI-SM blend ratios), barrel temperature, and screw speed, for the development of texturized pea-shiitake mushroom (TPSM) protein with improved textural properties; and (2) to characterise the chemical and functional properties of the resulting TPSM. While previous studies have extensively investigated the extrusion of soy and wheat proteins, research on optimising extrusion conditions for pea proteins, particularly in combination with edible mushrooms such as shiitake mushrooms, remains limited. The globular structure of pea protein presents challenges in achieving a well-defined fibrous texture, requiring further exploration of processing conditions and ingredient combinations to enhance texture and functionality. This research addresses these gaps by characterising the chemical and functional attributes of TPSM, contributing to sustainable food production and advancing green processing technologies. The findings may support the commercial application of alternative plant-based protein sources while providing insights into the impact of extrusion processing on protein structure and functionality.

2. Materials and Methods

2.1. Raw Materials

A commercial PPI with a protein content of 80.46% on dry matter basis was sourced from Gogrand Resources, Shah Alam, Selangor, Malaysia. Fresh sliced SM, cultivated and packaged by Fungo Malaysia Sdn. Bhd. and commercially produced wheat flour, obtained from Syarikat Faiza Sdn. Bhd. were from a local market in Shah Alam, Selangor, Malaysia. PPI and fresh SM were utilized as the primary ingredients, with wheat flour serving as a secondary component in the development of TPSM.

2.2. Chemicals and Reagents

The chemicals and reagents that were used in this research were 0.5% potassium hydroxide (KOH), 1.25% and 98% sulfuric acid (H_2SO_4), Kjeldahl catalyst tablets, 1.25%, 40%, 0.1 M, 1 M, and 4 M sodium hydroxide (NaOH), 4% boric acid (H_3BO_3), 1%, 0.1 M, 1 M, and 6 M hydrochloric acid (HCl), petroleum ether (C_6H_{14}), bumping chips, albumin standard, Bovine Serum Albumin (BSA), ninhydrin and Bradford reagent, 20 mM phosphate buffer, sodium citrate buffer (pH 2.2), 1 M sodium borate buffer (pH 9), tryptophan solutions, 24 mM and 25mM sodium acetate, 0.02% sodium azide (pH 6), and acetonitrile. All chemicals and standards were of analytical grade and were supplied by BT Science Sdn. Bhd., Cheras, Selangor, Malaysia.

2.3. Experimental design of extrusion conditions

RSM was employed using Minitab software (version 21.3, Minitab Inc., State College, PA, USA) to examine the relationship between process variables and response parameters. The BBD was selected to optimize extrusion conditions based on the methodology described by Mazaheri Tehrani et al. [26], with some modifications. The experimental design incorporated both process and categorical variables.

The independent variables include feed mixture composition (PPI-SM blend ratios), barrel temperature, and screw speed, each assessed at three levels (-1, 0, 1), as detailed in **Error! Reference source not found.** The coded values and their corresponding experimental ranges were determined based on preliminary trials and the extrudability of the extruder. The findings indicated that, at a moisture content of 45%, the feed mixture could be effectively extruded when PPI-SM blends in proportions ranging from 10-35%. This was achieved within barrel temperature and screw speed ranges of 130-150°C and 110-160 rpm, respectively.

A total of 15 experimental runs, including three replicates at the central point, were conducted (**Error! Reference source not found.**). The response variables, integrity index (II) and water absorption capacity (WAC) were used to assess extrudate quality. The II reflects the degree of texturization and fiber formation, while WAC provides insights into the swelling behavior and water retention capacity of the product, contributing to its juiciness upon rehydration.

2.4. Preparation of TPSM

2.4.1. Processing of shiitake mushroom

SM were processed following the method described by Husain and Huda-Faujan [27], with slight modifications. Freshly sliced SM were thoroughly washed with clean water to remove surface impurities. The washed mushrooms were then air-dried on a sieve for 30 min to eliminate excess surface moisture. To maintain consistency with their original moisture content before washing, the mushrooms were further dried in a cabinet dryer at 60°C for 1 h to reduce excess moisture absorbed during washing, achieving an approximate moisture content of 90%. The dried mushrooms were then chopped using an electric chopper for 1 min to achieve a uniform texture.

2.4.2. Preparation of feed mixtures

A base mixture was prepared by blending PPI with SM, with wheat flour (2%) incorporated as a minor ingredient on a weight percentage basis. The mixture was blended for 5 min using a kitchen hand mixer at 1000 rpm to achieve homogeneity. Prior to extrusion, the feed mixture was stored in sealed containers at 4°C, as described by Mazlan et al. [28] and Webb et al. [29].

2.4.3. Preconditioning of feed mixtures

Preconditioning of the feed mixtures was conducted following the method described by Sue Shan et al. [30] to introduce the feed moisture into PPI-SM mixtures before extrusion, as per experimental design. The moisture content of the feed mixtures was determined by drying each sample at 105°C until a constant weight was achieved, following the AOAC [31] method. To achieve the 45% moisture levels, distilled water was gradually added in small increments (approximately 5 mL at a time) with continuous mixing using a kitchen hand mixer to ensure homogeneity and prevent clumping. After mixing, the feed mixtures were equilibrated by storing them at 4°C for 24 h to allow for moisture equilibration before extrusion. The required amount of water was calculated using the following equation [13]:

$$\text{Amount of water to add (mL)} = \left[\frac{100 - \% \text{ actual moisture content in feed mixtures}}{(100 - \% \text{ desired moisture content in feed mixtures})} - 1 \right] \times \text{amount of dry feed mixtures (g)} \quad (1)$$

2.4.4. Extrusion process

The TPSM was prepared following the method described by Mazlan et al. [28], with minor modifications. The PPI-SM blends were texturized using a laboratory-scale single-screw Brabender 19/20D extruder (Brabender GmbH and Co., Duisburg, Germany), which featured a grooved barrel, a screw length-to-diameter (L/D) ratio of

20:1, two heating zones, and a heating element at the die head. A 20 x 2 mm (width x height) slit die was used for extrusion.

The process was conducted under varying conditions specified in the 15 experimental runs generated by RSM, as shown in **Error! Reference source not found.**, to determine the optimal extrusion conditions for TPSM production. Fixed extrusion variables included 45% feed moisture content, 20 rpm feeder speed, feeding zone temperature of 80°C, and die zone temperature of 45°C. A compression screw with a 2:1 compression ratio was used to extrude the mixture. After the extrusion process, TPSMs were collected, cooled to ambient temperature, and dried at 50°C for 24 h in a cabinet dryer. The dried TPSM samples were stored in plastic zipper bags at 25°C until further analysis.

2.5. Preparation of Texturized Pea Protein (TPP)

A feed mixture of PPI (major ingredient) and 2% wheat flour (minor ingredient) was prepared following the method described in Section 2.4.2 and 2.4.3. TPP was produced from PPI following the procedure outlined in Section 2.4.4, using a laboratory-scale single-screw Brabender 19/20D extruder (Brabender GmbH and Co., Duisburg, Germany). The extruder was carried out under optimized extrusion conditions, with screw speed of 151.41 rpm and a barrel temperature (zone 2) set to 150°C.

2.6. Determination of physical properties of TPSM as response variable for optimization analysis

2.6.1. Integrity index (II)

Integrity index (II) was determined using the method described by Brishti et al. [13]. A 3 g of TPSM sample was immersed in 100 mL of distilled water in a beaker and placed in a water bath at 80°C for 30 min. After soaking, the sample was autoclaved at 121°C for 15 min, followed by rinsing with distilled water for 15 sec. The hydrated sample was subsequently homogenised in 100 mL of distilled water at 15,000 rpm for 1 min using an IKA-Werke ULTRA-TURRAX® T25 homogenizer (IKA-Werke GmbH & Co. KG, Staufen, Germany). The homogenised sample was filtered through a 20-mesh sieve and dried in an oven (Memmert GmbH + Co. KG, Schwabach, Germany) at 105°C until equilibrium moisture content was achieved. The II% was calculated using the following formula:

$$\text{Integrity index (\%)} = \frac{\text{Dry residue weight of sample (g)}}{\text{Initial sample weight (g)}} \times 100 \quad (2)$$

2.6.2. Water absorption capacity (WAC)

Water absorption capacity (WAC) was determined according to the method outlined by Ma et al. [32]. A 5 g of dried TPSM sample was rehydrated in 100 mL of distilled water for 2 h at 80°C. After rehydration, the sample was drained at room temperature for 5 min using a 20-meshes screen before being weighed. The WAC (%) was using the following equation:

$$\text{WAC (\%)} = \left[\frac{(W_2 - W_1)}{W_1} \right] \times 100 \quad (3)$$

where W_1 represents the sample weight before rehydration, and W_2 represents the weight after rehydration.

2.7. Determination of chemical and functional properties of TPSM

2.7.1. Protein content

The protein content of TPSM was determined following the standard procedure outlined by AOAC [33] using the Kjeldahl method ($N \times 6.25$). A 0.6 g of the sample was used for protein analysis. The percentage of Kjeldahl nitrogen was calculated using the following equation:

$$\text{Kjeldahl nitrogen, \%} = \frac{[(V_S - V_B) \times M \times 14.01]}{W \times 10} \quad (4)$$

The crude protein content (%) was then determined using the equation:

$$\text{Crude protein, \%} = \% \text{ Kjeldahl N} \times F \quad (5)$$

where, V_S = volume (mL) of standardized acid used to titrate the sample; V_B = volume (mL) of standardized acid used for the reagent blank; M = molarity of standard HCl; 14.01 = atomic weight of N; W = weight (g) of test portion or standard; 10 = factor to convert mg/g to %; and F = factor to convert N to protein (6.25).

2.7.2. Total amino acids

The total amino acid content was determined following the method described by Wang et al. [34] and Li et al. [35]. About 2 mg of protein isolates and extrudates were hydrolysed in 4 mL of 6 M HCl at 110°C for 24 h in sealed tubes under nitrogen. After hydrolysis, the samples were cooled to room temperature and filtered through a cellulose filter paper to remove precipitates. The filtrate was diluted with deionised water to a final volume of 50 mL, followed by the addition 1 mL of sodium citrate buffer (pH 2.2). The solution was further filtered using a syringe filter (0.22 µm pore size) before analysis.

Tryptophan was analysed using high-performance liquid chromatography (HPLC) following basic hydrolysis. Hydrolysates were cooled down on ice, neutralized to pH 7 with NaOH, and diluted to 25 mL with 1 M sodium borate buffer (pH 9). Aliquots of these solutions were filtered through a 0.45 µm Millex filters (Millipore) before injection. Standard tryptophan solutions were prepared by diluting a stock solution (0.51 mg tryptophan/ml 4 M NaOH) to 3 mL with 4 M NaOH and incubated in oven at 100°C for 4 h. Then, 20 µl samples were injected into the column. An isocratic elution system consisting of 25 mM sodium acetate, 0.02% sodium azide (pH 6)/acetonitrile (91:9) delivered at 0.9 ml/min was used.

Amino acids were quantified after derivatisation with 0.8 µL of diethyl ethoxymethylenemalonate, using D, L- α -aminobutyric acid as the internal standard. The reaction was conducted at 50°C for 50 min with vigorous shaking. The resulting mixture was cooled to room temperature and 15 µL was injected into the chromatograph. Chromatographic resolution of a mixture of the derivatives of seventeen amino acids, including proline and cystine, was achieved within 35 min using a binary gradient system with solvents A (24 mM sodium acetate containing 0.02% of sodium azide, pH 6) and solvent B (acetonitrile). The gradient program proceeded at a flow-rate of 0.9 mL/min as follows: 0-3 min, linear gradient from A-B (91:9) to A-B (86:14); 3-13 min, elution with A-B (86:14); 13-30 min, linear gradient from A-B (86:14) to A-B (69:31); 30-35 min, elution with A-B (69:31).

The analysis was performed using a reversed-phase column (Navopack C18, 4 µm; Waters, Milford, MA, USA) with dimensions of 300mm × 3.9mm i.d. The column was maintained at 18°C during analysis, and detection was performed at 280 nm.

2.7.3. Protein solubility

Protein solubility was evaluated over a pH range of 1-11, following the method distributed by Boye et al. [36], with modifications. Briefly, 100 mg of the protein sample was dispersed in 10 mL of distilled water, and the pH was adjusted using 1 M HCl or 1 M NaOH. The mixtures were stirred continuously for 30 min, followed by centrifugation at 3000 rpm for 30 min. The protein concentration in the supernatant was determined using the Bradford method, measuring absorbance at 595nm with bovine serum albumin (BSA) as the standard protein. Total protein content was determined as described in Section 2.7.1. Protein solubility (%) was calculated using the following formula:

$$\text{Protein solubility (\%)} = \left(\frac{\text{soluble protein in the supernatant}}{\text{total protein in the samples}} \right) \times 100 \quad (6)$$

The solubility profile was obtained by plotting the average protein solubility of triplicate samples against pH.

2.7.4. Sodium dodecyl sulfate-polyacrylamide gel electrophoresis (SDS-PAGE)

The molecular weight distribution of proteins in the samples was determined using sodium dodecyl sulfate-polyacrylamide gel electrophoresis (SDS-PAGE), following the method of Wang et al. [34]. A Mini-PROTEAN®

3 Electrophoresis Unit (Bio-Rad, Hercules, CA, USA) and Criterion™ TGX™ Precast Any kD Gel (Catalog No. 5671124, Bio-Rad) were utilised for analysis. Protein samples (2.5 mg) were dissolved in 1 mL of Laemmli buffer (0.1 M Tris-Tricine, pH 6.8, containing 2% SDS, 5% β-mercaptoethanol, and 0.025% bromophenol blue), stirred for 1 h, boiled for 5 min, centrifuged at 10,000 × g for 1 min, and loaded onto the gel. Each well contained 20 µg of protein premixed with Stained Protein Standard. Electrophoresis was conducted at 150 V, and the gel was subsequently stained with 0.125% Coomassie Brilliant Blue R-250 in a solution of 7% acetic acid and 40% methanol (v/v). Destaining was performed using a solution of 7% acetic acid and 30% ethanol (v/v). Precision Plus Protein™ standards (10–250 kDa, Bio-Rad, Hercules, CA, USA) were used as molecular weight markers.

2.7.5. Water- and oil absorption capacity

WAC was determined following the method described in Section 2.6.2. Oil absorption capacity (OAC) was measured following the method outlined by Hong et al. [18], with minor modification. A 1 g of ground sample was mixed with 10 mL refined corn oil in a pre-weighed 15 mL centrifuge tube. Oil slurries were manually agitated for 2 min, allowed to stand at room temperature for 30 min, and then centrifuged at 3500 rpm for 30 min. The clear supernatant was carefully decanted and discarded, and any remaining oil droplets adhering to the tube were removed using cotton wool. OAC was calculated as follows:

$$\text{OAC} \left(\frac{\text{g oil}}{\text{g sample}} \right) = \frac{W_2 - W_1 - W_0}{W_0} \quad (7)$$

where W_1 is the weight of the centrifuge tube with the dry sample, W_2 is the weight of the tube after oil decantation, and W_0 is the weight of the dry sample.

2.7.6. Foaming properties

Foaming capacity (FC) and foaming stability (FS) were assessed according to the method described by Brishti et al. [7], with slight modifications. A 3 g of ground sample was mixed with 100 mL of distilled water and homogenised at high speed for 5 min at room temperature. The homogenised mixture was transferred to a 250 mL measuring cylinder, and the foam volume was recorded at 30 sec to calculate FC%, while the foam volume after 30 min was recorded to calculate FS%.

FC(%) was calculated as follows:

$$\text{Foaming capacity (\%)} = \frac{\text{Vol. after whipping (mL)} - \text{Vol. before whipping (mL)}}{\text{Vol. before whipping (mL)}} \times 100 \quad (8)$$

FS(%) was determined using:

$$\text{Foaming stability (\%)} = \frac{\text{Foam vol. after time (t)}}{\text{Initial foam vol.}} \times 100 \quad (9)$$

2.7.7. Emulsifying properties

Emulsion capacity (EC) and emulsion stability (ES) were determined following the method described by Brishti et al. [7], with minor modifications. A 2 g of ground sample was mixed with 20 mL of distilled water and 20 mL of corn oil in a centrifuge tube. EC% was calculated as the volume increase of the emulsion layer after being centrifuged at 3500 rpm for 25 min. While ES% was determined by measuring the emulsion volume after incubation at 80°C for 30 min, followed by centrifugation under the same conditions.

EC (%) calculations were as follows:

$$\text{Emulsion capacity (\%)} = \frac{\text{Volume of the emulsion layer (mL)}}{\text{Volume of the whole layer (mL)}} \times 100 \quad (10)$$

ES (%) was calculated as:

$$\text{Emulsion stability (\%)} = \frac{\text{Volume of the emulsion layer after heating (mL)}}{\text{Volume of the whole layer (mL)}} \times 100 \quad (11)$$

2.7.8. Gelling properties

The least gelling concentration (LGC) of the pulse protein isolates and extrudates was evaluated based on the procedure outlined by Boye et al. [36]. Suspensions were prepared by dissolving appropriate amounts of ground sample in 5 mL of deionized water to achieve concentrations ranging from 2–20% (w/v). The suspensions were vortexed, sealed in test tubes, and heated at 100°C in a water bath for 60 min. After heating, the tubes were rapidly cooled under tap water and stored at 4°C overnight. Gelling ability was assessed by inverting the tubes, where a firm gel was noted when the suspension did not flow upon inversion, while a weak gel was identified if a semi-solid that partially flowed was observed. The LGC was defined as the minimum concentration at which a self-supporting gel was formed. All tests were conducted in duplicate.

2.8. Optimization, model validation, and statistical analysis

Experimental data for all response variables were analysed using Minitab software (version 21.3). A significance level of 95% ($p < 0.05$) was applied to determine the statistical significance of findings. A second-order polynomial equation was used to model the experimental data, expressed as follows:

$$Y = \beta_0 + \beta_1 X + \beta_2 B + \beta_3 S + \beta_{12} XB + \beta_{13} XS + \beta_{23} BS + \beta_{11} X^2 + \beta_{22} B^2 + \beta_{33} S^2 \quad (12)$$

where, Y = response, X = feed mixtures (%), B = barrel temperature (°C), S = screw speed (rpm), β_0 = intercept, $\beta_1, \beta_2, \beta_3$ correspond to the linear terms, interaction regression coefficients are represented by $\beta_{12}, \beta_{13}, \beta_{23}$ while quadratic terms are denoted by $\beta_{11}, \beta_{22}, \beta_{33}$.

The adequacy of the experimental model was evaluated using the coefficient of determination (R^2) and regression coefficients. Response surface and contour plots were generated based on the regression equations to visualize the effects of independent variables. Analysis of variance (ANOVA) was conducted in Minitab to assess the significance of independent variables on the response outcomes. A numerical multi-response optimizer was applied to determine the optimal processing conditions for developing TPSM. This approach predicted the combination of independent variable levels that would yield the most desirable TPSM properties.

Further statistical analyses were performed using SPSS software (version 28, SPSS Inc., Illinois, USA). Independent t-tests and one-way were conducted, applying a significance level of $p < 0.05$. When significant differences were identified among means, the least significant difference (LSD) multiple comparison test was used. Data were reported as mean \pm standard deviation (SD), with all experiments conducted in triplicate. For multiple mean comparisons, Tukey's test was applied at a 5% significance level.

3. Results and discussion

The experimental results for the II and WAC of the TPSM are summarized Table 1. Table 2 presents the regression coefficients and ANOVA results ($p < 0.05$) for TPSM. To evaluate the combined effects of two treatment factors, response surface plots were generated using two independent variables while keeping the third variables, deemed the least significant, is kept constant at its central level [32]. Figures 1 and 2 illustrate the relationship between the independent variables and the response parameters, providing a comparison of the effects.

Table 1 Response surface design with coded and actual levels of extrusion parameters.

Run	X (%)	B (°C)	S (rpm)	II (%)	WAC (%)
1	-1 (10)	-1 (130)	0 (135)	0.00	225.57
2	1 (35)	-1 (130)	0 (135)	40.00	165.16
3	-1 (10)	1 (150)	0 (135)	17.16	259.44
4	1 (35)	1 (150)	0 (135)	68.55	129.94
5	-1 (10)	0 (140)	-1 (110)	2.77	246.13
6	1 (35)	0 (140)	-1 (110)	50.39	148.42

7	-1 (10)	0 (140)	1 (160)	5.81	248.91
8	1 (35)	0 (140)	1 (160)	55.97	140.60
9	0 (22.5)	-1 (130)	-1 (110)	5.86	216.33
10	0 (22.5)	1 (150)	-1 (110)	43.87	194.93
11	0 (22.5)	-1 (130)	1 (160)	23.10	192.00
12	0 (22.5)	1 (150)	1 (160)	42.67	208.39
13	0 (22.5)	0 (140)	0 (135)	33.31	188.31
14	0 (22.5)	0 (140)	0 (135)	39.34	183.08
15	0 (22.5)	0 (140)	0 (135)	33.26	189.81

X=Feed mixtures; *B*=Barrel temperature; *S*=Screw speed; *II*=Integrity index; *WAC*=Water absorption capacity.

Table 2 Analysis of variance at $p<0.05$ and regression coefficients for *II* and *WAC* expressed in full quadratic models.

Factors	II		WAC	
	Coefficients	<i>p</i> -Value	Coefficients	<i>p</i> -Value
Regression		0.000		0.000
Linear		0.000		0.000
Squares		0.140		0.011
Interaction		0.098		0.001
Constant	35.30	0.000	187.07	0.000
<i>X</i>	23.65	0.000	-49.49	0.000
<i>B</i>	12.91	0.000	-0.80	0.555
<i>S</i>	3.03	0.045	-1.99	0.175
<i>X</i> * <i>X</i>	-2.01	0.293	0.53	0.786
<i>B</i> * <i>B</i>	-1.87	0.325	7.43	0.010
<i>S</i> * <i>S</i>	-4.56	0.045	8.42	0.006
<i>X</i> * <i>B</i>	2.85	0.144	-17.27	0.000
<i>X</i> * <i>S</i>	0.63	0.715	-2.65	0.197
<i>B</i> * <i>S</i>	-4.61	0.038	9.45	0.003
<i>R</i> ²		99.12%		99.71%
<i>R</i> ² -adj		91.41%		96.91%
Lack of fit		0.595		0.528
<i>f</i> -value		0.81		1.02

The values ($p<0.05$) mean they are significantly different. *X*=Feed mixtures; *B*=Barrel temperature; *S*=Screw speed; *II*=Integrity index; *WAC*=Water absorption capacity.

3.1. Integrity index (*II*)

II measures the structural quality of rehydrated, pressurized, dispersed, and dried texturized protein samples, reflecting the yield and quality of TPSM. A higher *II* indicates reduced solid loss and increased structural strength, suggesting greater protein texturization which improves product quality. In TLP production, higher protein denaturation fosters the formation of insoluble proteins that contribute to a fibrous, meat-like texture, an essential characteristic for meat extender products [13,37,38].

The *II* values for TPSM ranged from 0–68.55%, as presented in Table 3 and the regression model explained 99.12% of the variation ($R^2 = 99.12\%$). The lack-of-fit value of 0.595 further confirms the adequacy of the model. The coded regression equation for *II* is given by:

$$\begin{aligned}
 \text{II (\%)} = & -981 - 0.99X + 8.50B + 4.63S - 0.0129X^2 - 0.0187B^2 - 0.00730S^2 + 0.0228XB + 0.00203XS \\
 & -0.01844BS
 \end{aligned}
 \tag{13}$$

Response surface plot (Fig. 1) depict the effects of two independent variables on *II* while maintaining the third variable at its central level. Analysis of these plots reveals that all linear factors, quadratic term for screw speed (S^2), and the interaction between barrel temperature and screw speed (*BS*) significantly ($p<0.05$) affect *II*. As presented in Figure 1(a), *II* increased with higher PPI and SM feed mixture ratios as well as elevated barrel

temperature, with the highest II recorded at 35% SM feed mixture and a barrel temperature of 150°C. Under constant screw speed conditions, increasing feed mixture ratios similarly enhanced II, as shown in Figure 1(b), where the highest value was observed at 35% SM feed mixture and a screw speed of 133.16 rpm. This outcome suggests that TPSM may be less susceptible to extreme processing conditions [39].

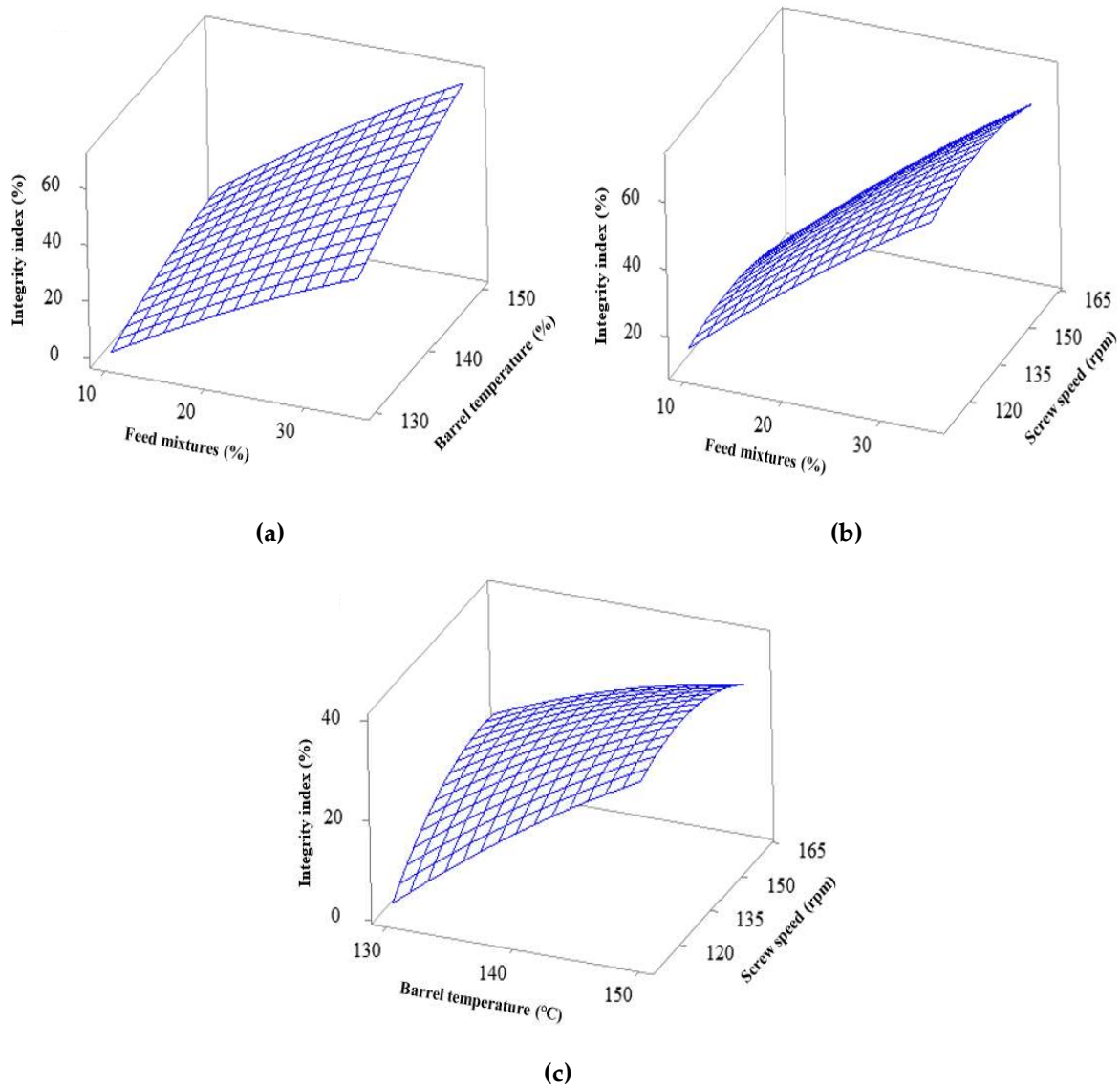


Fig. 1 Response surface plots showing the effects of independent variables on the II of TPSM: (a) Variation of II with feed mixture and barrel temperature, with screw speed held constant; (b) Variation of II with feed mixture ratio and screw speed, with barrel temperature held constant; (c) Variation of II with barrel temperature and screw speed, with feed mixture ratio held constant.

The increased II observed with higher SM concentrations may be attributed to SM's polysaccharide content, which supports protein-protein and protein-polysaccharide interactions that reinforce the fibrous structure [19,40]. These results align with findings by Samard et al. [41], where the combination of soy protein isolates and wheat gluten significantly enhanced II compared to formulation without wheat gluten, highlighting the role of feed mixture composition in improving structural integrity and quality of TLP. Similarly, Lei et al. [42] reported that blending multiple materials, such as walnut protein (WP) with wheat gluten (WG), stabilised the protein network during extrusion, facilitating stronger hydrophobic interactions and hydrogen bonding, alongside disulphide bond formation, which are essential for reinforcing the fibrous structure [43,44].

Regarding extrusion parameters, a higher screw speed and barrel temperature also increased II (Fig. 1(c)). This observation supports previous research indicating that elevated barrel temperatures and rapid screw speeds enhance protein cross-linking and molecular rearrangement, thereby improving fibrous structure and increasing II [45]. Comparable findings were reported by Wang et al. [44], who found that increased extrusion temperatures significantly modified potato protein structure, improving cross-linking, reducing protein solubility, and enhancing structural strength. Similarly, Brishti et al. [13] reported that barrel temperature and screw speed affected the deformation properties of mung bean protein isolates. The optimal conditions for achieving high II were determined to be a barrel temperature of 150°C and a screw speed of 130 rpm (Fig. 1(c)), consistent with the findings of Maurya and Said [46] regarding TLP hardness.

These results confirm that careful control of extrusion parameters and feed mixture composition (10-35% SM, 130-150°C, 110-160 rpm) is critical for optimising the integrity index of TPSM. The dominant influence of feed mixture ratios, together with the significant contributions from screw speed and barrel temperature, emphasises the importance of formulation in achieving optimal texturization.

3.2. Water absorption capacity (WAC)

WAC indicates the amount of water that TLP structures can absorb and retain after rehydration. This property significantly influences the texture, juiciness, and mouthfeel of the product, all of which are critical for consumer acceptance. Generally, a higher WAC is desirable for texturized protein products [13]. In this study, the WAC values of TPSM ranged from 129.94–259.44% (Table 3). The highest WAC was observed at a 90:10 PPI:SM feed mixture ratio, a barrel temperature of 150°C, and a screw speed of 135 rpm. The regression model explained 99.71% of the WAC variation ($R^2 = 99.71\%$), with a lack of fit value of 0.528, confirming the adequacy of the model. The regression equation for WAC is:

$$\text{WAC (\%)} = 2254 + 16.38X - 22.87B - 8.82S + 0.0034X^2 + 0.0743B^2 + 0.01347S^2 - 0.1382XB - 0.0084XS + 0.03779BS \quad (14)$$

Response surface plots (Fig. 2) illustrate the individual and interactive effects of the independent variables on WAC. Among the independent variables, the feed mixtures composition exhibited the most significant influence ($p < 0.05$) on WAC, followed by the quadratic effects of barrel temperature (B^2) and screw speed (S^2). Additionally, the interaction effects between feed mixtures and barrel temperature (XB), as well as between barrel temperature and screw speed (BS), also significantly affected WAC.

The variations in WAC observed across different extrusion conditions for TPSMs can be attributed to changes in protein-water interactions and the structural modifications induced by the extrusion process [37]. Figure 2(a) and Figure 2(b) show that reducing the proportion of SM in the feed mixture, particularly at higher barrel temperatures and screw speeds, lead to increased WAC. The highest WAC was recorded with a 90:10 PPI:SM ratio, a barrel temperature of 150°C, and a screw speed of 160 rpm. These findings emphasize the critical role of both SM content and extrusion parameters on WAC. In agreement with the Maningat et al. [20] and Agathian et al. [47], the results indicate that higher proportions of PPI contribute to improved WAC, although the exact values depend on the interplay between feed composition and extrusion conditions.

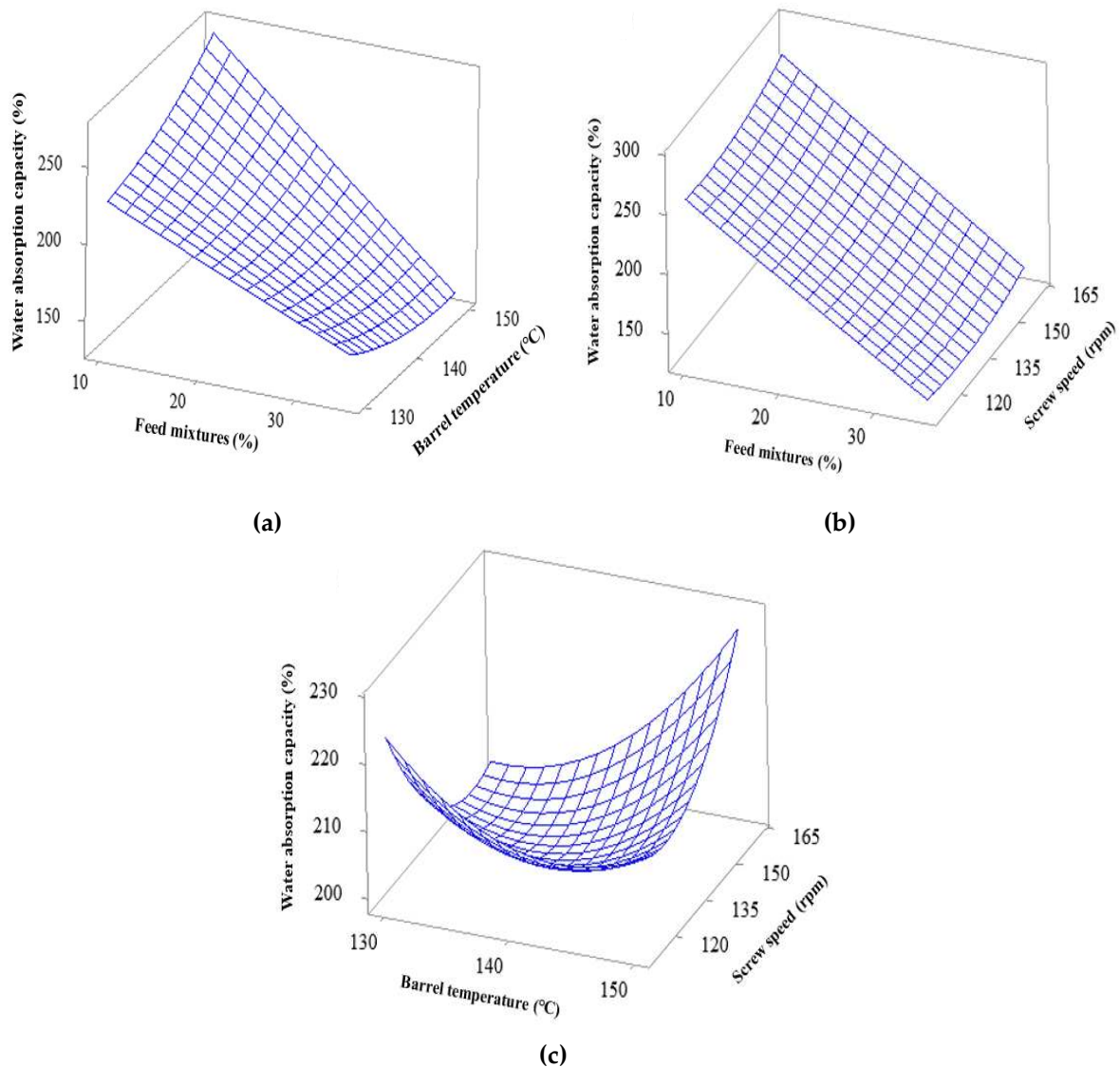


Fig. 2 Response surface plots showing the effects of independent variables on the WAC of TPSM: **(a)** Variation of WAC with feed mixture and barrel temperature, with screw speed held constant; **(b)** Variation of WAC with feed mixture ratio and screw speed, with barrel temperature held constant; **(c)** Variation of WAC with barrel temperature and screw speed, with feed mixture ratio held constant.

The combined effects of barrel temperature and screw speed were found to positively influenced the WAC of TPSM, as shown in Figures 3(c). When comparing extreme extrusion settings, the highest WAC (227.47%) was obtained at the maximum setting (150°C and 160 rpm) due to rapid expansion of blends that promotes pore formation within the TPSM matrix [13,48], while lower extrusion setting resulted in a slightly reduced WAC (222.55%). This observation reinforces the importance of optimising both barrel temperature and screw speed to enhance WAC, as supported by Enobong and Madu [49], who found that higher barrel temperatures and screw speeds improve WAC in extruded products. Although some studies [32,46] suggest minimal effects of screw speed on rehydration, the present findings demonstrate a clear synergistic effect between barrel temperature and screw speed. This interaction underscores the importance of optimizing both parameters to achieve superior rehydration properties [26].

During extrusion, protein unfolding exposes hydrophilic groups, promoting greater water interaction and improved hydration properties. Structural modifications induced by extrusion, particularly at elevated temperatures, enhance WAC properties by disrupting non-covalent and disulphide bonds, thereby improving the fibrous network's ability to retain water [43,44]. Similarly, Lei et al. [42] observed that WP-WG blends exhibited

improved fibrous structures through enhanced bonding strength and hydrophobic interactions, contributing to superior WAC. These findings align with the present study, where higher barrel temperatures and reduced SM content promoted improved water retention through enhanced protein bonding.

These findings confirm that optimising extrusion conditions, particularly feed mixture ratios and extrusion parameters, can significantly enhance the WAC of TPSM. This outcome is consistent with previous research [13,37] on other plant-based protein blends (e.g. navy-pinto bean, defatted soy flour, soy-wheat starch and mung bean) which also demonstrated improved WAC when extrusion conditions were optimized. Overall, this study highlights the vital role of barrel temperature in determining WAC in TPSM.

3.3. Optimisation and validation of RSM models

This study aimed to optimise the development of TPSM for its potential use as a meat extender in vegetarian meals by enhancing its physical properties, specifically the II and WAC. The optimisation process involved adjusting the feed mixture ratio of PPI and SM (X), along with key extrusion parameters, such as barrel temperature (B), and screw speed (S). The objective was to identify processing conditions that maximise both II and WAC of the TPSM. Table 5 presents the predicted and experimental values for these responses. The optimal conditions were determined as follows: a feed mixture ratio of 80.91% PPI and 19.09% SM, screw speed of 151.41 rpm, and barrel temperature of 150°C. Under these conditions, the extruded TPSM exhibited an II and WAC values of $35.77 \pm 0.95\%$ and $219.21 \pm 5.84\%$, respectively (Table 5).

Validation experiments were conducted under these optimal conditions, and all responses were measured. A one-sample t-test was applied to assess the accuracy of the response surface model by comparing predicted and experimental values. The results showed no significant differences ($p > 0.05$) between the predicted and observed data, as shown in Table 5. Further, the reliability of the model was confirmed by a coefficient of variation below 5% and coefficients of determination (R^2) ranging from 99.12% to 99.71% for II and WAC, indicating that the model effectively explained the variation in these responses.

Table 3 Comparison between experimental and predicted values of physical properties of TPSM.

Physical properties	Experimental value	Predicted value
Integrity index (%)	35.77 ± 0.95	35.89 ± 0.00
Water absorption capacity (%)	219.21 ± 5.84	220.95 ± 0.00

In conclusion, the optimised processing parameters were validated as effective for producing TPSM with desirable physical properties. This study provides a valuable reference for future research on the optimisation of II and WAC in protein-rich materials ($\geq 80\%$ protein content) derived from PPI blended with other plant-based ingredients such as SM. Future work should explore broader ranges of processing conditions and incorporate sensory evaluations to fully assess consumer acceptance and scalability for industrial applications.

3.4. Characterization on chemical and functional properties of TPSM

3.4.1. Protein content

The protein composition of the analysed samples is presented in Table 6. The results indicate that the protein content of TPSM was significantly lower ($p < 0.05$) than that of TPP. Similarly, the protein content of the PPI-SM blend was significantly reduced compared to PPI alone. Notably, extrusion led to a significant decrease in the protein content of TPP, whereas TPSM exhibited a substantial increase in protein content relative to its raw material.

Protein is critical for the formation of TLP, with concentrations between 50–70% generally required to achieve fibrous structures during extrusion. Pea protein is known to achieve fibrous textures at relatively lower concentrations compared to other plant proteins, which explains its frequent use in pea-based TLPs, while soy-based TLPs are often produced using protein concentrates [18]. Previous studies have reported that TPP generally contains the highest protein levels, reported between 62.4-76.6%, followed by pea-navy bean (66.2%) and pea-chickpea (68.3%) blends combinations. In contrast, textured soy protein has a relatively lower protein content,

ranging from 50-55.8% [18,50]. Despite these differences, both pea and soy proteins are widely employed in TLP production due to their functional properties, including gelation, emulsification, and water retention. In this study, TPSM exhibited a protein content of $73.49 \pm 0.26\%$, which aligns with previously reported ranges for pea-based TLPs and reflects the influences of extrusion on enhancing protein content in TPSM relative to its raw material.

Variations in protein content following extrusion may be attributed to differences in intermolecular interactions. Protein texturisation primarily involves the formation and disruption of disulphide bonds and non-covalent interactions, such as hydrogen bonds, van der Waals forces, and hydrophobic interactions. Major chemical bonds, such as peptide bonds, generally remain unaffected during extrusion [15,43,46]. The influence of these bonds can vary depending on the protein source. Pea protein has been shown to form stable networks through disulphide bonds and intermolecular hydrogen bonding, which enhances aggregation and stabilises fibrous structures [10]. Conversely, soy protein exhibits stronger disulphide bonding alongside hydrophobic and electrostatic interactions, contributing to denser matrices during extrusion [15].

The reduced protein content observed in TPSM compared to TPP may be attributed to differences in bond strength and protein aggregation dynamics, due to the presence of SM, which contains polysaccharides that could influence protein solubility and dispersion during extrusion. Such effects may have contributed to reduced protein recovery in TPSM. Previous research indicates that protein-polysaccharide blends are prone to phase separation, which promotes the formation of fibrous layers rather than homogeneous mixtures during extrusion [19,40,43]. This behaviour may have influenced TPSM's texturisation characteristics in this study.

While amino acid composition significantly influences protein functionality, the distinct structural properties of PPI, TPP, and TPSM are likely to have influenced their respective texturisation behaviours. Protein molecules, composed of diverse amino acid units, are subject to multiple bonding interactions that can either facilitate or hinder the formation of stable fibrous structures. Given that the extrusion process imposes simultaneous thermal and mechanical stresses, conventional protein-protein interaction mechanisms may be partially disrupted [43]. Further analysis of the amino acid profiles of these samples is presented in Section 3.4.2.

Table 4 Protein content of pea protein isolate and its extrudates.

Protein samples	Protein content (%)
PPI + SM blends	54.53 ± 0.25^d
PPI	80.46 ± 0.24^a
TPP	78.44 ± 0.20^b
TPSM	73.49 ± 0.26^c

Mean \pm s.d. in column followed by different letters are significantly ($p < 0.05$) different.

3.4.2. Total amino acids

The amino acid composition of TPSM, TPP, and PPI provided insights into the impact of extrusion and feed mixtures on protein quality. As shown in Table 7, TPSM maintained a balanced amino acid composition after extrusion, comparable to TPP, with no significant reduction ($p > 0.05$) in total amino acid content. This outcome suggests that the optimised extrusion conditions effectively preserved amino acid integrity, aligning with findings by Osen et al. [51]. Essential amino acids (EAA) accounted for 42.61% of the total amino acid content in TPSM, meeting the nutritional requirements set by WHO/FAO/UNU [3]. TPSM exhibited a well-balanced amino acid profile comparable to TPP, with notably high concentrations of aspartic acid, glutamic acid, arginine, leucine, lysine, and phenylalanine, collectively accounting for 59.46% of the total amino acids. However, cystine and methionine levels were relatively low (<2%).

The EAA content in TPSM has been found to be higher than in texturized soy protein, mung bean, and peanut protein [52]. Although extrusion processing can degrade EAA due to excessive heat exposure, potentially reducing amino acids such as Met, Cys, Lys, Arg, Tyr, and Leu [3], the present study observed only minor reductions in lysine levels, with decreases of 3.41% and 2.73% in TPSM and TPP, respectively, with no statistically significant difference. This underscores the importance of optimised extrusion parameters in minimising nutrient losses. Previous studies have reported lysine as the most thermally unstable EAA during extrusion, with degradation rates

ranging from 10% to 49% due to its free ϵ -amino group, Maillard reactions and its interaction with reducing sugars [13,52]. Notably, the lysine content in TPSM is comparable to that in texturized soy protein concentrate, highlighting its potential as a high-quality plant-based protein source [52]. Given that amino acid losses are directly related to the intensity of the extrusion process, it is crucial to carefully regulate time and temperature to preserve the protein quality of legume-based extrudates [3,51].

Among the analysed amino acids, glutamic and aspartic acids were predominant in all samples, with TPSM exhibiting the significantly highest ($p<0.05$) glutamic acid content. This trend aligns with observations reported by Osen et al. [51] and Samard and Ryu [52], who identified glutamic and aspartic acids as the most abundant amino acids in soy protein isolates (ISP) and various legume proteins, including extruded soybean/corn flour, mung bean, and peanut proteins. The levels of sulphur-containing amino acids (Cys and Met) and acid-stable amino acids (Lys, Arg, and Phe) decreased after extrusion in both PPI and PPI-SM blends, aligning with the results of Osen et al. [51]. However, in TPSM, the sulphur-containing amino acids did not differ significantly from TPP ($p>0.05$), but there was a significant difference compared to PPI ($p<0.05$).

Table 5 Amino acid content (g/100g protein) of pea proteins isolate and extrudates produced under optimum conditions.

Amino acids (g/100g protein)	PPI	TPP	TPSM
Polar			
Cystine ^S	0.61 ± 0.07 ^a	0.57 ± 0.01 ^{ab}	0.54 ± 0.01 ^b
Serine	2.76 ± 0.00 ^a	3.50 ± 0.09 ^a	3.45 ± 0.52 ^a
Threonine ^E	3.87 ± 0.02 ^a	3.80 ± 0.00 ^b	3.83 ± 0.03 ^{ab}
Tyrosine	3.03 ± 0.00 ^a	2.91 ± 0.01 ^b	2.95 ± 0.02 ^b
Electrically charged			
Aspartic acid	11.19 ± 0.04 ^a	11.30 ± 0.01 ^a	11.34 ± 0.07 ^a
Glutamic acid	16.68 ± 0.02 ^b	16.64 ± 0.21 ^b	17.37 ± 0.07 ^a
Arginine ^a	8.87 ± 0.03 ^a	8.63 ± 0.02 ^b	8.65 ± 0.06 ^b
Histidine ^E	2.36 ± 0.01 ^b	2.58 ± 0.04 ^a	2.38 ± 0.08 ^{ab}
Lysine ^{E a}	7.33 ± 0.01 ^a	7.13 ± 0.02 ^b	7.08 ± 0.02 ^b
Non-polar			
Alanine	4.67 ± 0.02 ^a	4.54 ± 0.04 ^b	4.64 ± 0.00 ^a
Glycine	4.33 ± 0.00 ^a	4.30 ± 0.01 ^{ab}	4.29 ± 0.00 ^b
Isoleucine ^E	5.29 ± 0.01 ^a	5.12 ± 0.03 ^b	5.26 ± 0.01 ^a
Leucine ^E	9.08 ± 0.03 ^a	8.82 ± 0.04 ^b	9.00 ± 0.01 ^a
Methionine ^{E S}	1.25 ± 0.00 ^a	1.17 ± 0.02 ^a	1.16 ± 0.04 ^a
Phenylalanine ^{E a}	6.05 ± 0.01 ^a	5.85 ± 0.00 ^b	6.02 ± 0.01 ^a
Proline	4.83 ± 0.12 ^{ab}	5.33 ± 0.05 ^a	4.17 ± 0.33 ^b
Valine ^E	5.87 ± 0.01 ^{ab}	5.77 ± 0.02 ^b	5.93 ± 0.04 ^a
Tryptophan ^E	1.96 ± 0.04 ^a	2.09 ± 0.04 ^a	1.98 ± 0.05 ^a
Hydrophilic	56.68 ± 0.08 ^a	57.03 ± 0.10 ^a	57.56 ± 0.47 ^a
Hydrophobic	43.32 ± 0.09 ^a	42.97 ± 0.10 ^a	42.44 ± 0.47 ^a
Essential amino acids	43.05 ± 0.05 ^a	42.30 ± 0.13 ^b	42.61 ± 0.07 ^b
Sulfur amino acids	1.85 ± 0.00 ^a	1.74 ± 0.01 ^{ab}	1.70 ± 0.05 ^b
Acid-stable amino acids	22.26 ± 0.05 ^a	21.60 ± 0.04 ^b	21.75 ± 0.02 ^b
Total amino acids	100.00 ± 0.00 ^a	100.00 ± 0.00 ^a	100.00 ± 0.00 ^a

Mean ± s.d. in row followed by different letters are significantly ($p<0.05$) different.

^E Essential amino acids. ^S Sulfur-containing amino acids. ^a Acid-stable amino acids.

While Samard and Ryu [52] reported an increase in sulphur-containing amino acids post-extrusion, suggesting that intermolecular disulfide bonds contribute to stabilising protein structures during texturization, the present study observed minimal reductions in sulphur-containing amino acids in TPSM. This stability may be attributed to the formation of intermolecular disulphide bonds, which protect cystine and methionine during thermal processing [52]. Cystine and methionine were found to be limiting amino acids in PPI and its extrudates [53]. Disulphide bonds are essential for stabilising protein structure and enhancing resistance to heat-induced degradation. A study on EPP revealed that disulphide bond content decreased significantly when extrusion temperatures increased from 60–100°C, a phenomenon linked to bond breakage under elevated heat and pressure conditions, as disulphide bonds are generally stable only between 60–90°C [44]. The presence of SM may have contributed to this stability, given its bioactive compounds with antioxidant properties, which can mitigate oxidative stress during extrusion [19,24]. The synergistic effect between PPI and SM may have enhanced the interaction between hydrophobic interactions and hydrogen bonds, contributing to improved retention of sulphur-containing amino acids, similar with study on the extrudate from the blending of WP and WG [42].

Hydrophilic and hydrophobic amino acids, along with polar and non-polar amino acids, are essential for protein functionality, influencing solubility and water absorption [7]. In this study, TPSM reported a highest hydrophilic and lowest hydrophobic amino acid content among the samples. These differences are significant as hydrophilic amino acids enhance protein solubility, while hydrophobic amino acids contribute to protein aggregation and texturisation during the extrusion process [3]. The reduction in hydrophobic interactions may have resulted from the exposure of hydrophobic groups during the extrusion process, consistent with previous observations in EPP, where extreme extrusion conditions (>120°C) altered the protein structure and masked hydrophobic groups [44]. High retention rates of hydrophobic amino acids were observed for TPSM and TPP, with TPP showing 99.19% and 98.26%, respectively, and TPSM achieving 97.97% and 98.98%. These results indicate that the extrusion process and the inclusion of SM effectively preserved amino acid integrity, with minimal losses. Pea protein has often been compared to soy protein due to its balanced amino acid profile and functional properties. Although ISP exhibits the highest total hydrophilic amino acid content, PPI has the highest total hydrophobic amino acid content, followed by peanut and wheat gluten [52].

The well-balanced amino acid composition of TPSM highlights its potential as a functional protein source for meat alternatives, with minimal adverse effects from extrusion. These findings reinforce the importance of controlling processing conditions to preserve the nutritional quality of legume-based proteins, ensuring their suitability for high-protein applications.

3.4.3. Protein solubility

Protein solubility is primarily determined by the distribution and interaction of hydrophilic and hydrophobic amino acids within the protein structure. The distribution and proportion of these amino acids within a protein structure play a crucial role in determining solubility, which is a key functional property in assessing protein texturisation. Evaluating solubility across different pH levels provides insights into protein behaviour under various conditions, particularly in the context of TLP production [13]. The solubility profiles of PPI, PPI–SM blends, and their corresponding extrudates (TPSM and TPP) across a pH range of 1–11, as presented in Figure 3, are consistent with findings from previous studies.

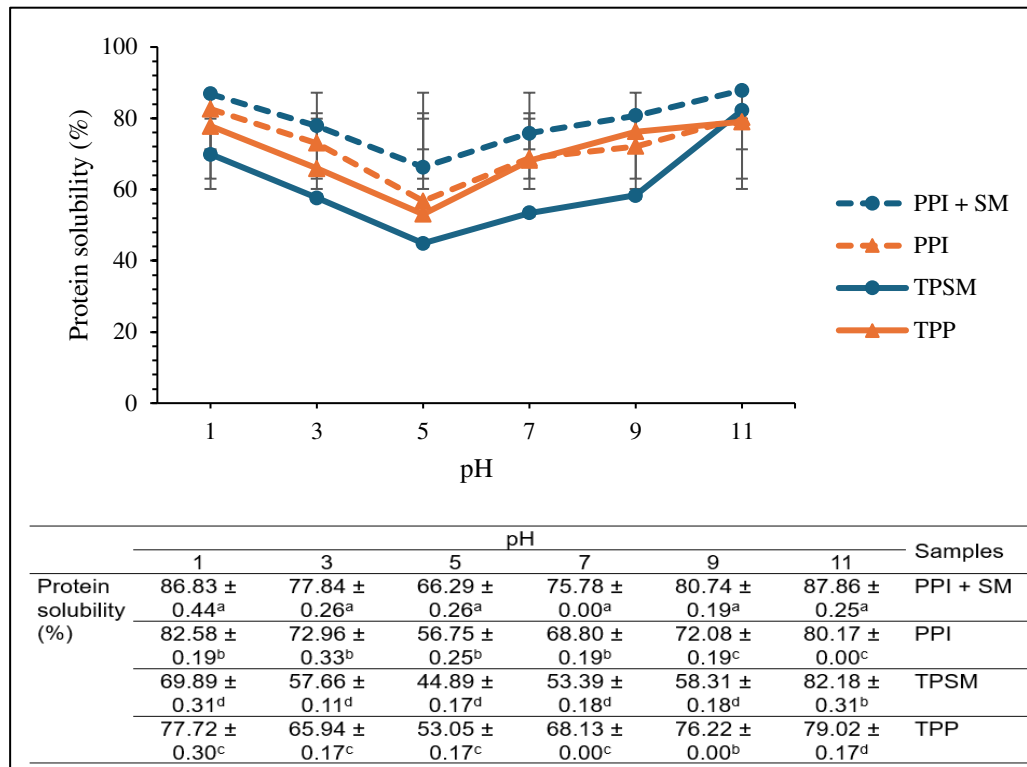


Fig. 3 Effect of pH on protein solubility of pea protein raw materials and its extrudates. Mean \pm s.d. in a column followed by different letters are significantly ($p < 0.05$) difference. PPI, pea protein isolate; SM, shiitake mushroom; TPP, Texturized Pea Protein; TPSM, Texturized Pea-Shiitake Mushroom.

The results indicate that TPSM and TPP exhibited significantly ($p < 0.05$) lower solubility than their respective raw materials. Across all samples, solubility decreased with increasing pH until reaching the isoelectric point (pH 5), where the lowest solubility was observed. Beyond this point, solubility increased with rising pH. These findings align with previous research, which reported that protein solubility is typically lowest between pH 4 and 5 due to the absence of electrostatic repulsion, leading to protein aggregation via hydrophobic interactions [10,52]. Conversely, at strongly acidic (pH 1 and 3) or alkaline (pH 9 and 11) conditions, solubility was significantly higher, which can be attributed to increased electrostatic repulsion and hydration of charged residues, facilitating protein dispersion [13].

PPI, known for its high protein content ($>80\%$), typically exhibits solubility ranging from 47% to 96%, depending on the pH [54]. The solubility of the PPI–SM blends was significantly higher across all pH levels compared to PPI alone (Fig. 3), suggesting that the presence of SM enhanced solubility. This improvement may be attributed to the presence of hydrophilic components in SM, which contribute to better water interaction. However, extrusion significantly reduced solubility in TPSM and TPP compared to their native forms across all pH values, indicating enhanced texturization. Notably, TPSM exhibited a greater reduction in solubility than TPP, suggesting a more pronounced structural transformation [52]. Since protein solubility is inversely related to texturisation, these findings reinforce the effectiveness of SM incorporation in PPI-based TLPs.

Extrusion-induced changes in protein solubility are primarily governed by alterations in intermolecular bonding. Xiao et al. [55] reported that extrudates derived from soy protein, pea protein, and WG exhibited markedly reduced solubility compared to their raw material blends, suggesting extensive aggregation and bond formation. Hydrophobic interactions were identified as the dominant force stabilising protein aggregates, followed by hydrogen bonding, while disulfide bonds played a crucial role in maintaining structural integrity. In particular, WG-containing samples exhibited the most pronounced solubility decline, indicating a greater contribution of disulfide bonds to network stabilisation. These findings align with previous reports, where Osen et al. [51] and

Zhang and Ryu [56] observed variations in bonding mechanisms across different protein systems, highlighting the dependence of solubility on both formulation and processing conditions.

The relationship between extrusion temperature and protein solubility further supports the role of bond formation in structural changes. Wang et al. [44] demonstrated that solubility in EPP declined following extrusion. However, at temperatures exceeding 120°C, solubility increased, suggesting the breakdown of non-covalent and disulfide bonds, leading to aggregate dissociation. Similarly, Lei et al. [42] found that WG incorporation reduced solubility, reinforcing its role in strengthening protein networks via disulfide bond formation. Collectively, these findings indicate that disulfide bonds primarily stabilise the texturised protein structure, with hydrophobic interactions and hydrogen bonding contributing to aggregate formation.

Overall, these results demonstrate that extrusion effectively modifies protein solubility by promoting structural aggregation through disulfide bonds, hydrophobic interactions, and hydrogen bonding. The observed differences between TPSM and TPP highlight the influence of formulation on bond formation and texturisation. These findings further underscore the importance of optimising extrusion conditions to achieve desirable texturised protein structures in plant-based meat products.

3.4.4. Molecular weight distribution (SDS-PAGE)

Extrusion processing disrupts protein structures by denaturing them and weakening the stabilizing forces that maintain their tertiary and quaternary conformations [13]. To investigate these changes, SDS-PAGE analysis was conducted to investigate these structural changes by separating and analysing protein profiles based on molecular weight after extraction [40]. This study employed SDS-PAGE to assess how extrusion influenced the protein structure of TPSM in comparison to PPI (prior to extrusion) and TPP, highlighting the role of SM in mitigating protein denaturation. Both reducing and non-reducing conditions were applied to observe structural modifications. Reducing agents such as dithiothreitol (DTT) or β -mercaptoethanol were used to disrupt disulfide bonds, enabling the separation of proteins based on their primary structure and molecular weight. In contrast, non-reducing conditions preserved disulfide bonds, maintaining the proteins' higher-order structures [57].

Figure 4 presents the SDS-PAGE spectra for PPI and its extruded forms. Lane 1 displays the molecular weight marker, while lanes 2 through 7 show the profiles of TPSM, TPP, and PPI. Pea proteins primarily consist of legumin (L), vicilin (V), and convicilin (CV). Under reducing conditions, disulfide bonds in legumin (approximately 60 kDa) were cleaved, resulting in distinct bands at approximately 40 kDa ($L\alpha$) and 20 kDa ($L\beta$) [51]. The protein profile indicate that the extrusion process and the inclusion of SM considerably influence the protein structure within the TPSM formulation. Figure 5 indicates the molecular weights of proteins at six distinct bands: 75 kDa (legumin, Rf 0.174), 50 kDa (convicilin, Rf 0.287), 37 kDa (legumin acidic subunit, Rf 0.387), 25 kDa (legumin, Rf 0.554), 20 kDa (legumin basic subunit, Rf 0.619), and 15 kDa (vicilin, Rf 0.771).

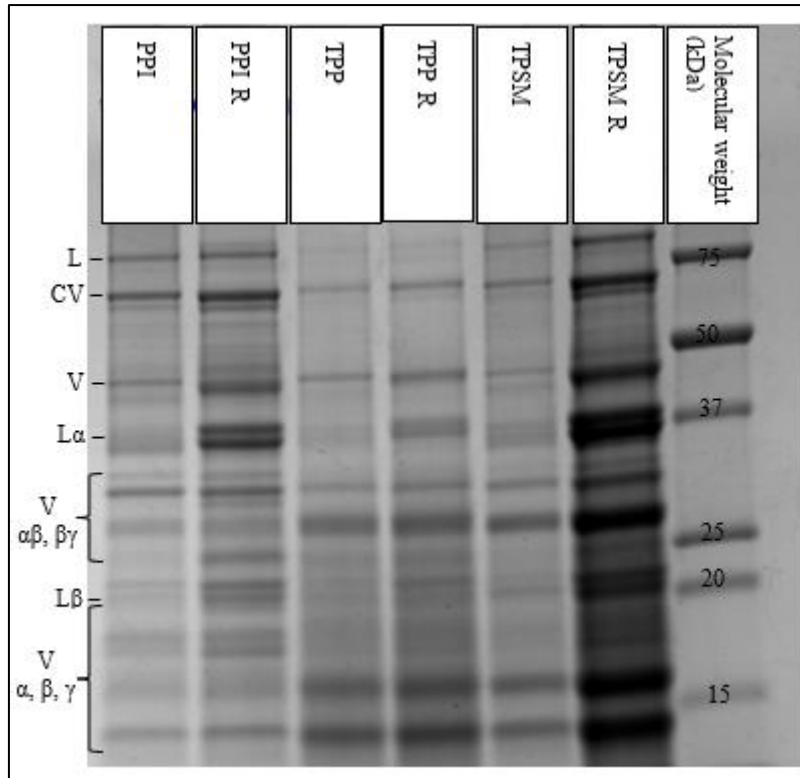


Fig. 4 Sodium dodecylsulphate-poly-acrylamide gel electrophoresis (SDS-PAGE) pattern (10% acrylamide, 60 μg protein on gel) of protein samples under reducing (R) and non-reducing conditions. PPI, pea protein isolate; TPP, texturized pea protein; TPSM, texturized pea-shiitake mushroom; V, vicilin; L, legumin; L α , legumin acidic subunit; and L β , legumin basic subunit.

SDS-PAGE profiles of extrudates revealed notable changes in band patterns, intensities, and molecular weight distributions compared to raw PPI, which can be attributed to the combined effects of extrusion and the inclusion of SM blends [48]. From Figure 4, PPI displayed 15 major bands with molecular weights ranging from 12.3 to 75.0 kDa. After extrusion (TPP), nine bands were detected, with molecular weights between 12.2 and 64.9 kDa. In contrast, TPSM displayed 14 bands, spanning 12.7 to 84.1 kDa. These findings suggest that extrusion and SM incorporation influenced the concentration and visibility of protein bands, as reported by Hidayat et al. [40]

Proteins extracted from TPP exhibited diminished intensities, indicating that extrusion caused significant denaturation. This denaturation led to the unfolding and rearrangement of proteins into smaller molecules, which may have eluted during electrophoresis due to the gel's porosity. Alternatively, aggregation of proteins into larger macromolecules might have rendered them too large to penetrate the gel pores, leading to undetectable bands. These outcomes align with studies on protein cross-linking in extruded wheat, whey, mung bean, and pea proteins [13,51]. In contrast, the inclusion of SM resulted in partial unfolding of protein structures without significant alterations in molecular weight distribution, likely due to controlled depolymerization during extrusion [13].

Under non-reducing conditions, legumin bands, which were distinct in PPI, disappeared in TPP, likely due to insolubilization caused by disulfide cross-linking and participation in macromolecular networks [58]. However, these cross-linked structures were broken under reducing conditions, as evidenced by the appearance of L α and L β subunits. Vicilin and convicilin bands persisted in both TPP and TPSM, regardless of the conditions, indicating their limited role in disulfide bond formation and network structures [51]. Non-globulin fractions were not discernible, confirming that PPI primarily comprises globulins, irrespective of SM addition [59]. The findings suggest that TPSM experienced fewer structural changes during extrusion due to the protective effects of SM blends, in contrast to TPP, which showed extensive protein denaturation.

These findings align with recent studies on molecular weight modifications in extruded proteins. Wang et al. [44] demonstrated that high extrusion temperatures led to significant protein degradation in EPP, resulting in

lighter protein bands due to the breakdown of smaller molecular weight subunits. Similarly, Lei et al. [42] investigated WP-WG mixtures during high-moisture extrusion cooking. Their study found that WP degraded into smaller fragments in the melting zone, while WG exhibited extensive aggregation and macromolecular assembly during cooling.

Both studies highlight the need to optimise extrusion conditions to balance protein breakdown and aggregation, ensuring desirable structural and functional properties in plant-based protein products. The protective role of SM in TPSM supports this approach, as its inclusion moderated protein denaturation, contributing to improved structural integrity compared to TPP.

3.4.5. Water- and oil absorption capacity

WAC and OAC are critical functional properties that influence the texture, juiciness, and sensory characteristics of food products. Higher WAC and OAC can minimise processing losses, reduce greasiness, and enhance the overall palatability of food [16]. These properties are primarily determined by the strength of intermolecular bonds, which influence protein structure, porosity, and hydrophobicity following extrusion. Additionally, they serve as key indicators of structural modifications occurring during processing, affecting moisture retention and the suitability of proteins for various formulations [55].

Table 8 presents the WAC and OAC values for PPI, TPSM, and TPP. Across all protein samples, WAC values were consistently higher than OAC values, regardless of extrusion treatment or the inclusion of SM. PPI and TPSM exhibited significantly greater WAC ($p < 0.05$) than TPP, whereas TPSM had lower OAC compared to both TPP and PPI. These variations suggest that SM influences the protein network structure formed during extrusion, affecting the ability of proteins to retain water and interact with oil [52]. Additionally, these results highlight the role of protein solubility and interfacial interactions in improving the functional properties of plant-based proteins for applications such as comminuted meat products [13]. The differences in WAC and OAC can be attributed to variations in the availability of polar and non-polar amino acids, as shown in Table 7.

Since fresh meat is inherently high in moisture, TLPs must exhibit substantial WAC to replicate the texture, juiciness, and chewiness of conventional meat products [60]. As shown in Table 8, WAC for TPP was significantly ($p < 0.05$) lower than for PPI, whereas no significant difference ($p < 0.05$) was observed between TPSM and PPI. This suggests that while extrusion reduces WAC in PPI, the addition of SM can counteract this effect. The higher WAC observed in TPSM is likely due to a higher concentration of hydrophilic amino acids, which enhance water retention. The ability of TLPs to retain water appears to be influenced more by the abundance of polar amino acids than by overall protein content. During extrusion, protein denaturation and restructuring contribute to the formation of a protein matrix, improving water entrapment [18]. Post-extrusion, protein–water interactions are likely strengthened, further enhancing WAC [16]. Additionally the inclusion of SM, a rich source of insoluble dietary fibre, may also contribute to higher WAC, as polysaccharides facilitate water retention and improve textural properties in processed foods [19,40]. These observations align with studies by Xiao et al. [55], who reported that a high PPI content in extrudates leads to a denser, less porous matrix, thereby restricting water absorption. The observed reduction in WAC following extrusion suggests that excessive protein hydration before processing may weaken intermolecular hydrogen bonds and compromise the integrity of the porous matrix. Moreover, the decline in WAC correlates with increased springiness and chewiness, as stronger protein–protein interactions contribute to a more rigid network.

OAC is primarily influenced by the presence of hydrophobic groups on protein surfaces, which determine the extent of protein–lipid interactions. Protein denaturation during extrusion alters hydrophobicity, leading to variations in OAC [26]. In this study, TPSM exhibited lower OAC (0.87 ± 0.02 g/g) than TPP (0.96 ± 0.03 g/g) and PPI (1.06 ± 0.03 g/g), suggesting a lower concentration of hydrophobic amino acids in TPSM, as indicated in Table 7. A similar reduction in OAC following extrusion has been reported in previous studies, where heat treatment modified the hydrophobic properties of PPI [52]. Higher protein concentrations tend to increase OAC, as elevated levels of hydrophobic amino acids lead to greater exposure of non-polar sites, allowing for stronger protein–oil interactions [18]. The observed increase in OAC may be attributed to protein denaturation, which disrupts electrostatic and hydrogen bonding, thereby allowing non-polar residues to interact more readily with oil

molecules. Additionally, the porous microstructure of extrudates may further contribute to oil entrapment [55]. The lower OAC in TPSM may be attributed to the reduced availability of non-polar amino acids, thereby limiting lipid interactions.

In summary, WAC and OAC are influenced by multiple factors, including protein composition, denaturation levels, and the extent of protein interactions with water and oil [61]. WAC reflects the protein's ability to interact with water at a molecular level, while OAC depends on interactions with oil. Proteins, possess both hydrophilic and hydrophobic regions, which undergo structural modifications during extrusion. The exposure of hydrophilic groups enhances WAC, while the presence of hydrophobic groups on the protein surface contribute to higher OAC values [26,52]. TLPs with higher WAC are more suited for moisture-retentive applications, such as soups and gravies, whereas those with elevated OAC may be preferable for products like sausages, salad dressings, and meat extenders. Understanding the role of extrusion in modifying plant protein properties can aid in tailoring formulations for specific applications in the development of high-quality plant-based meat products [55]. These findings suggest that the inclusion of SM in TLPs can improve water retention without significantly altering oil absorption, which may have implications for the texture and sensory properties of plant-based meat analogues.

Table 6 Functional properties of pea protein isolate and extruded protein.

Functional properties	PPI	TPSM	TPP
Water absorption capacity (%)	228.02 ± 8.62 ^a	219.21 ± 5.84 ^a	154.32 ± 6.86 ^b
Oil absorption capacity (g/g)	1.06 ± 0.03 ^a	0.87 ± 0.02 ^c	0.96 ± 0.03 ^b
Foaming capacity (%)	12.67 ± 1.15 ^a	4.00 ± 2.00 ^b	5.33 ± 1.15 ^b
Foaming stability (%)	95.87 ± 0.98 ^b	100 ± 0.00 ^a	98.74 ± 1.09 ^a
Emulsion capacity (%)	55.21 ± 1.80 ^a	56.25 ± 0.00 ^a	56.17 ± 0.14 ^a
Emulsion stability (%)	55.21 ± 1.80 ^a	56.25 ± 0.00 ^a	55.21 ± 1.80 ^a

Mean ± s.d. in row followed by different letters are significantly ($p < 0.05$) different.

3.4.6. Foaming properties

Foaming properties, including foaming capacity (FC) and foaming stability (FS), are essential functional characteristics of proteins, particularly in food formulations. FC refers to a protein's ability to generate foam, while FS indicates its capacity to maintain foam structure over time [35]. Proteins that efficiently adsorb onto the air-liquid interface and undergo structural rearrangement at this interface typically exhibit superior foaming properties compared to those with slower adsorption or resistance to unfolding [7]. Table 8 presents the FC and FS values for TPSM, TPP, and PPI.

The results indicate that FC in PPI decreased significantly ($p < 0.05$) after extrusion, irrespective of the inclusion of SM. This reduction suggests that the extrusion process alters the structural conformation of proteins, affecting their ability to form foam [36]. The decline in FC may be attributed to the disruption of intermolecular interactions, particularly hydrogen bonds and hydrophobic interactions, which play a crucial role in maintaining protein structure. Consequently, the exposure and rearrangement of hydrophilic groups at the protein surface reduce surface activity, slowing adsorption at the air-liquid interface and thereby diminishing foam formation [44,62]. Since FC is often correlated with protein solubility, the observed reduction in FC in extruded samples aligns with the decrease in protein solubility seen in TPP and TPSM [35]. This trend is consistent with findings from previous studies, where the extrusion of plant proteins, including PPI, SPI, and WG, resulted in substantial reductions in FC due to thermal denaturation and increased protein aggregation [55].

Extrusion-induced structural modifications influence intermolecular bond strength, further contributing to changes in foaming behaviour. Proteins that maintain high solubility and flexible molecular structures typically exhibit better foaming properties due to their ability to rapidly migrate to the interface and stabilise foam films. However, extrusion promotes the formation of more stable protein aggregates through intensified hydrophobic interactions and disulfide cross-linking, which enhances protein-protein interactions at the expense of interfacial stabilisation. This phenomenon has been reported in EPP, where FC decreased with higher extrusion temperatures exacerbating the decline [44]. These reductions are largely attributed to the irreversible thermal denaturation and structural rigidity induced by mechanical shearing, leading to impaired foam formation and stability [16].

In contrast, FS showed an opposite trend. After 30 minutes of standing time, FS for PPI was recorded at $95.87 \pm 0.98\%$, which was lower than that of TPP ($98.74 \pm 1.09\%$) and TPSM ($100 \pm 0.00\%$). This indicates that extrusion significantly enhanced FS ($p < 0.05$), with TPSM exhibiting the highest stability. This improvement is likely due to the formation of protein aggregates during extrusion, which contribute to a more cohesive interfacial network that strengthens foam stability. Under high temperature and shear conditions, peptide chains unfold, reconfigure, and interact via intra- and intermolecular forces, forming a cohesive two-dimensional network at the air-liquid interface that enhance FS [7,35,62]. The increased FS observed in TPSM and TPP suggests that the restructured protein matrix is more resistant to foam collapse, reinforcing its potential application in stabilised food emulsions.

The inclusion of SM in TLPs did not significantly affect foaming properties, indicating that SM contributes minimally to enhancing FC or FS. This implies that factors such as protein unfolding and molecular rearrangement during extrusion exert a more substantial impact on foaming behaviour than the presence of SM. Nonetheless, while the reduction in FC may limit the use of extruded proteins in aerated food systems, the improved FS observed in TPSM highlights its potential for applications requiring enhanced foam stability.

3.4.7. Emulsifying properties

Emulsifying properties are essential functional attributes of proteins, particularly in processed meat products, where they influence texture, stability, and sensory characteristics. Proteins aid in emulsification by reducing surface tension at the oil-water interface and forming a protective layer around oil droplets to prevent aggregation [16]. These properties are typically assessed through emulsion capacity (EC), which measures a protein's ability to form emulsions, and emulsion stability (ES), which reflects its ability to maintain these emulsions over time. Table 8 presents the EC and ES values for TPSM, TPP, and PPI.

The results indicate that no significant differences ($p > 0.05$) were observed in emulsifying properties among the protein samples. This finding is consistent with Singh and Koksel [63], who reported similar emulsification behaviour in extruded soybean meal. However, the results contrast with those of Zhang et al. [62], Téllez-Morales et al. [64], Wang et al. [44], and Xiao et al. [55], who observed notable variations in emulsifying properties depending on processing conditions. Zhang et al. [62] reported a notable improvement in the emulsifying properties of PPI when extruded under specific conditions, particularly at moisture contents ranging from 30% to 60%. In contrast, Wang et al. [44] and Téllez-Morales et al. [64] documented a decline in the emulsifying properties of extruded yellow pea flour, potato protein, PPI, SPI, and WG, attributing the reduction to protein aggregation and decreased solubility.

The reduction in emulsifying capacity was attributed to lower solubility and surface hydrophobicity, reinforcing previous findings that link solubility to interfacial activity. At moderate extrusion temperatures, protein unfolding increases the exposed surface area, improving adsorption at the oil-water interface. However, as temperature rises further, protein aggregation and refolding diminish emulsifying efficiency. The reduced exposure of aromatic residues weakens protein affinity for the oil-water interface, while decreased charged amino acid content lowers electrostatic repulsion between oil droplets, thereby reducing emulsion stability [44]. These findings highlight how extrusion-induced protein denaturation, aggregation, and charge redistribution significantly influence emulsifying properties. Additionally, variations in sample formulation, extrusion processing conditions, and extruder type (single- or twin-screw) modulate these effects, demonstrating the complexity of extrusion-induced modifications in protein functionality [55].

Although the observed differences in EC and ES were not statistically significant, TPSM exhibited a slight improvement in emulsification following extrusion and the incorporation of SM. The thermal and mechanical stresses encountered during extrusion likely altered protein secondary structures, leading to partial denaturation and unfolding. This process facilitates the formation of smaller peptides and free amino acids, which, upon homogenisation, expose hydrophobic groups that interact with oil molecules while hydrophilic groups interact with water. This interaction forms a stabilising film around oil droplets, enhancing emulsion stability [62].

Changes in protein solubility due to extrusion may also influence emulsification. Singh and Koksel [63] suggested that reduced solubility following extrusion could negatively impact emulsifying properties. However,

despite the lack of significant differences among samples, the ability of TPSM to stabilise emulsions suggests that it remains suitable for applications in comminuted meat products and as a meat extender. Given that higher EC contributes to improved texture, juiciness, and overall sensory quality in processed foods [7,39], TPSM may offer potential advantages in meat analogues and other food formulations.

3.4.8. Gelling properties

The ability of food proteins to form gels upon heating is a crucial functional property that influences food formulation and processing. The LGC is a widely used parameter to assess a protein's gelling ability, particularly for thermogelation, which reflects the structural transformations occurring during extrusion. LGC is defined as the lowest protein concentration at which a stable gel forms upon heating, preventing flow when the test tube is inverted. A lower LGC value indicates a stronger gel-forming capacity, making it a key parameter in evaluating protein structuring mechanisms during extrusion. This property is crucial for characterising proteins and understanding differences in their structural and functional behaviour. The formation of fibrous and layered structures in TLP during extrusion relies on heat, pressure, and shear-induced gelation [7,29,36,55].

The gelling properties of PPI and extruded proteins (TPP and TPSM) are summarized in Table 9. Among the protein samples, PPI exhibited superior gelation ability, with an LGC of 18% (w/v), which is consistent with values reported for commercial PPI (16–20%) and slightly higher than those documented in other studies (5.5–14.5%) [29,55,59]. In contrast, TPP and TPSM did not form gels at concentrations ranging from 2% to 20% (w/v), suggesting that extrusion significantly altered their gelling properties of protein samples. This trend is consistent with findings by Xiao et al. [55], who reported that texturised sample derived from blends of SPI, PPI, and WG exhibited increased LGC values at 50-60%, reinforcing the notion that aggregation and protein structural rearrangement during extrusion modulate intermolecular interactions critical for gel formation.

Table 7 Gelling behaviour of legume protein isolate and extruded protein at different concentration.

Concentration (% w/v)	Legumes		
	PPI	TPP	TPSM
2	∅∅	∅∅	∅∅
4	∅∅	∅∅	∅∅
6	∅∅	∅∅	∅∅
8	∅∅	∅∅	∅∅
10	∅∅	∅∅	∅∅
12	∅∅	∅∅	∅∅
14	±±	∅∅	∅∅
16	√±	∅∅	∅∅
18	√√	∅∅	∅∅
20	√√	∅∅	∅∅

∅ – No gel; ± - Weak gel; √± - Firm gel; and √√ - Least gelling protein concentration (LGC).

Post-extrusion, LGC values either increased or remained comparable to those of the raw materials, with texturised samples displaying values ranging from 19% to over 20%. The increase in LGC following extrusion was attributed to the formation of extensive protein aggregates, promoting the refolding of protein structures into compact conformations. This structural rearrangement restricted water absorption and hindered entrapment, thereby reducing gel network formation [55]. The disruption of protein structure during extrusion may have hindered gel formation in TPP and TPSM. Globular proteins, such as those in legumes, typically require moderate thermal unfolding to form a gel network [7]. However, the LGC test measures gelation under dilute conditions (12–20% solids), whereas protein structuring during high-moisture extrusion occurs at much higher solids content (60–70%) [29]. TLPs have been shown to exhibit favourable WAC, which may reduce protein aggregation during extrusion, leading to softer products with lower hardness, chewiness, and gel strength [65].

These findings suggest that extrusion processing has a significant impact on the gelling properties of legume proteins, with TPSM exhibiting reduced gelation ability after extrusion. Further research is needed to examine the gelling behaviour and %LGC of extruded proteins under varying processing conditions to provide a more

comprehensive understanding of protein gelation mechanisms and their relationship to extrusion-induced structural modifications.

4. Conclusion

This study successfully optimized the extrusion conditions for producing TPSM from PPI and SM using RSM, a BBD. The optimal extrusion parameters were determined as follows: feed mixture ratio of 80.91% PPI and 19.09% SM, screw speed of 151.41 rpm, and barrel temperature at 150°C. Among these parameters, barrel temperature had the most significant effect on the responses measured, followed by feed mixtures and screw speed. Both II and WAC improved with an increase in barrel temperature.

The chemical and functional characteristics of TPSM were evaluated and compared to PPI and TPP produced under identical optimal extrusion conditions. TPSM demonstrated favorable nitrogen and protein solubility indices, indicating significant texturization at its isoelectric point (pH 5). The product exhibited comparable water and oil absorption capacities, as well as foaming, emulsification, and gelling properties. However, TPSM displayed a lower rehydration capacity, requiring a longer time to achieve the desired softness. Although TPSM contained less protein than TPP, it maintained a well-balanced amino acid profile, particularly with higher lysine retention.

This study demonstrates the feasibility of producing high-quality texturized plant-based food products from PPI and SM. TPSM exhibits desirable functional and physicochemical properties, making it a promising candidate for addressing protein deficiencies. Additionally, TPSM holds significant potential as a meat extender, providing a healthier and more sustainable alternative to animal-based proteins. The findings underscore the opportunity to develop the next generation of plant-based protein products that align with both health and environmental goals.

Funding Declaration

This research was financially supported by Ministry of Higher Education (MOHE) under the Fundamental Research Grant Scheme (FRGS) (FRGS/1/2021/WAB04/UITM/02/1).

Clinical Trial Number

Not applicable. No clinical trial was conducted for this research.

References

1. Langyan, S., Yadava, P., Khan, F. N., Dae, Z. A., Singh, R., & Kumar, A. (2022). Sustaining protein nutrition through plant-based foods. *Frontiers in Nutrition*, 8, 772573. <https://doi.org/10.3389/fnut.2021.772573>
2. Chardigny, J.-M., & Walrand, S. (2016). Plant protein for food: Opportunities and bottlenecks. *OCL - Oilseeds, Fats, Crops and Lipids*, 23(4). <https://doi.org/10.1051/ocl/2016019>
3. Sá, A. G. A., Moreno, Y. M. F., & Carciofi, B. A. M. (2020). Plant proteins as a high-quality nutritional source for the human diet. *Trends in Food Science & Technology*, 97, 170–184. <https://doi.org/10.1016/j.tifs.2020.01.011>
4. Arueya, G. L., Owoosen, B. S., & Olatoye, K. K. (2017). Development of texturized vegetable protein from lima bean (*Phaseolus lunatus*) and African oil bean seed (*Pentaclethra macrophylla* Benth): Optimization approach. *Acta Universitatis Cibiniensis Series E: Food Technology*, 21(1), 61–68. <https://doi.org/10.1515/auaft-2017-0007>
5. Chaiwongsa, K., Charoenvitayavorakul, N., Pakasap, C., & Khuenpet, K. (2021). Effect of banana blossom substitution on quality characteristics of plant-based shiitake mushroom balls. *Asia-Pacific Journal of Science and Technology*, 26(3), 1–10.
6. Shanthakumar, P., Klepacka, J., Bains, A., Chawla, P., Dhull, S. B., & Najda, A. (2022). The current situation of pea protein and its application in the food industry. *Molecules*, 27(11), 5354.

7. Brishti, F. H., Zarei, M., Muhammad, S. K. S., Ismail-Fitry, M. R., Shukri, R., & Saari, N. (2017). Evaluation of the functional properties of mung bean protein isolate for development of textured vegetable protein. *International Food Research Journal*, 24(4), 1595–1605.
8. Kim, T. K., Yong, H. I., Cha, J. Y., Park, S. Y., Jung, S., & Choi, Y. S. (2022). Drying-induced restructured jerky analog developed using a combination of edible insect protein and textured vegetable protein. *Journal of Food Chemistry*, 373, 131519. <https://doi.org/10.1016/j.foodchem.2021.131519>
9. Rungruangmaitree, R., & Jiraungkoorskul, W. (2017). Pea, *Pisum sativum*, and its anticancer activity. *Pharmacognosy Reviews*, 11(21), 39–42. https://doi.org/10.4103/PHREV.PHREV_57_16
10. Vatansaver, S., Tulbek, C. M., & Riaz, M. N. (2020). Low- and high-moisture extrusion of pulse proteins as plant-based meat ingredients: A review. *Cereal Foods World*, 65(4). <https://doi.org/10.1094/cfw-65-4-0038>
11. Dahl, W. J., Foster, L. M., & Tyler, R. T. (2012). Review of the health benefits of peas (*Pisum sativum* L.). *British Journal of Nutrition*, 108(Suppl. 1). <https://doi.org/10.1017/S0007114512000852>
12. Lu, Z. X., He, J. F., Zhang, Y. C., & Bing, D. J. (2020). Composition, physicochemical properties of pea protein and its application in functional foods. *Critical Reviews in Food Science and Nutrition*, 60(15), 2593–2605. <https://doi.org/10.1080/10408398.2019.1651248>
13. Brishti, F. H., Chay, S. Y., Muhammad, K., Ismail-Fitry, M. R., Zarei, M., & Saari, N. (2021). Texturized mung bean protein as a sustainable food source: Effects of extrusion on its physical, textural, and protein quality. *Innovative Food Science & Emerging Technologies*, 67, 102591. <https://doi.org/10.1016/j.ifset.2020.102591>
14. Lee, J. S., Oh, H., Choi, I., Yoon, C. S., & Han, J. (2022). Physico-chemical characteristics of rice protein-based novel textured vegetable proteins as meat analogues produced by low-moisture extrusion cooking technology. *LWT - Food Science and Technology*, 157, 113056. <https://doi.org/10.1016/j.lwt.2021.113056>
15. Zhang, J., Liu, L., Liu, H., Yoon, A., Rizvi, S. S. H., & Wang, Q. (2018). Changes in conformation and quality of vegetable protein during texturization process by extrusion. *Critical Reviews in Food Science and Nutrition*, 59(20), 3267–3280. <https://doi.org/10.1080/10408398.2018.1487383>
16. Gao, Y., Sun, Y., Zhang, Y., Sun, Y., & Jin, T. (2022). Extrusion modification: Effect of extrusion on the functional properties and structure of rice protein. *Processes*, 10(9), 1–14. <https://doi.org/10.3390/pr10091871>
17. Kołodziejczak, K., Onopiuk, A., Szpicer, A., & Poltorak, A. (2022). Meat analogues in the perspective of recent scientific research: A review. *Foods*, 11(1), 105. <https://doi.org/10.3390/foods11010105>
18. Hong, S., Shen, Y., & Li, Y. (2022). Physicochemical and functional properties of texturized vegetable proteins and cooked patty textures: Comprehensive characterization and correlation analysis. *Foods*, 11(17), 2619. <https://doi.org/10.3390/foods11172619>
19. Yuan, X., Jiang, W., Zhang, D., Liu, H., & Sun, B. (2021). Textural, sensory, and volatile compounds analyses in formulations of sausage analogues elaborated with edible mushrooms and soy protein isolate as meat substitute. *Foods*, 11(1), 55. <https://doi.org/10.3390/foods11010052>
20. Maningat, C. C., Jeradechachai, T., & Buttshaw, M. R. (2022). Textured wheat and pea proteins for meat alternative applications. *Cereal Chemistry*, 99(1), 37–66. <https://doi.org/10.1002/CCHE.10503>
21. Sha, L., & Xiong, Y. L. (2020). Plant protein-based alternatives of reconstructed meat: Science, technology, and challenges. *Trends in Food Science & Technology*, 102, 51–61. <https://doi.org/10.1016/j.tifs.2020.05.022>
22. Chun, S., Chambers, E., & Chambers, D. H. (2020). Effects of shiitake (*Lentinus edodes* P.) mushroom powder and sodium tripolyphosphate on texture and flavor of pork patties. *Foods*, 9(5), 611. <https://doi.org/10.3390/foods9050611>
23. Das, A. K., Nanda, P. K., Dandapat, P., Bandyopadhyay, S., Gullón, P., Sivaraman, G. K., McClements, D. J., Gullón, B., & Lorenzo, J. M. (2021). Edible mushrooms as functional ingredients for development of healthier and more sustainable muscle foods: A flexitarian approach. *Molecules*, 26(9), 2463. <https://doi.org/10.3390/molecules26092463>

24. Kurek, M. A., Onopiuk, A., Pogorzelska-Nowicka, E., Szpicer, A., Zalewska, M., & Póltorak, A. (2022). Novel protein sources for applications in meat-alternative products—Insight and challenges. *Foods*, *11*(7), 957. <https://doi.org/10.3390/foods11070957>
25. Mohamad Mazlan, M., Talib, R. A., Mail, N. F., Taip, F. S., Chin, N. L., Sulaiman, R., Shukri, R., & Mohd Nor, M. Z. (2019). Effects of extrusion variables on corn-mango peel extrudates properties, torque and moisture loss. *International Journal of Food Properties*, *22*(1), 54–70. <https://doi.org/10.1080/10942912.2019.1568458>
26. Mazaheri Tehrani, M., Ehtiati, A., & Sharifi Azghandi, S. (2017). Application of genetic algorithm to optimize extrusion condition for soy-based meat analogue texturization. *Journal of Food Science and Technology*, *54*(5), 1119–1125. <https://doi.org/10.1007/s13197-017-2524-9>
27. Husain, H., & Huda-Faujan, N. (2020). Quality evaluation of imitation chicken nuggets from grey oyster mushroom stems and chickpea flour. *Malaysian Applied Biology*, *49*(3), 61–69. <https://doi.org/10.55230/mabjournal.v49i3.1542>
28. Mazlan, M. M., Talib, R. A., Chin, N. L., Shukri, R., Taip, F. S., Nor, M. Z. M., & Abdullah, N. (2020). Physical and microstructure properties of oyster mushroom-soy protein meat analog via single-screw extrusion. *Foods*, *9*(8), 1023. <https://doi.org/10.3390/foods9081023>
29. Webb, D., Plattner, B. J., Donald, E., Funk, D., Plattner, B. S., & Alavi, S. (2020). Role of chickpea flour in texturization of extruded pea protein. *Journal of Food Science*, *85*(12), 4180–4187. <https://doi.org/10.1111/1750-3841.15531>
30. Sue Shan, L., Sulaiman, R., Sanny, M., & Nur Hanani, Z. A. (2015). Effect of extrusion barrel temperatures on residence time and physical properties of various flour extrudates. *International Food Research Journal*, *22*(3), 965–972.
31. AOAC International. (2007). *Official methods of analysis of AOAC International* (18th ed.). Association of Official Analytical Chemists.
32. Ma, X., Gu, B., & Ryu, G. (2018). Optimization of extrusion variables for improving the qualities of textured vegetable protein with green tea using response surface methodology. *Food Engineering Progress*, *22*(1), 1–8. <https://doi.org/10.13050/foodengprog.2018.22.1.1>
33. AOAC International. (2000). *Official methods of analysis of AOAC International*. Association of Official Analytical Chemists International.
34. Wang, Y., Sánchez-Velázquez, O. A., Martínez-Villaluenga, C., Goycoolea, F. M., & Hernández-Álvarez, A. J. (2023). Effect of protein extraction and fractionation of chia seeds grown in different locations: Nutritional, antinutritional and protein quality assessment. *Food Bioscience*, *56*(August). <https://doi.org/10.1016/j.fbio.2023.103238>
35. Li, L., Huang, Y., Liu, Y., Xiong, Y., Wang, X., Tong, L., Wang, F., Fan, B., & Bai, X. (2023). Relationship between soybean protein isolate and textural properties of texturized vegetable protein. *Molecules*, *28*(22). <https://doi.org/10.3390/molecules28227465>
36. Boye, J. I., Aksay, S., Roufik, S., Ribéreau, S., Mondor, M., Farnworth, E., & Rajamohamed, S. H. (2010). Comparison of the functional properties of pea, chickpea and lentil protein concentrates processed using ultrafiltration and isoelectric precipitation techniques. *Food Research International*, *43*(2), 537–546. <https://doi.org/10.1016/j.foodres.2009.07.021>
37. Samard, S., Maung, T. T., Gu, B. Y., Kim, M. H., & Ryu, G. H. (2021). Influences of extrusion parameters on physicochemical properties of textured vegetable proteins and its meatless burger patty. *Food Science and Biotechnology*, *30*(3), 395–403. <https://doi.org/10.1007/s10068-021-00879-y>
38. Chan, E., Sinaki, N. Y., Rodas-González, A., Tulbek, M., & Koksel, F. (2024). Impact of protein blend formulation and extrusion conditions on the physical properties of texturised pea protein-extended beef burgers. *International Journal of Food Science and Technology*, *59*(2), 959–970. <https://doi.org/10.1111/ijfs.16856>

39. Chan, E., Rodas-González, A., Tulbek, M., & Koksel, F. (2024). Effects of protein formula and extrusion cooking conditions on the techno-functional properties of texturised pea proteins. *International Journal of Food Science and Technology*, 59(1), 584–595. <https://doi.org/10.1111/ijfs.16593>
40. Hidayat, B. T., Wea, A., & Andriati, N. (2017). Physicochemical, sensory attributes and protein profile by SDS-PAGE of beef sausage substituted with texturized vegetable protein. *Food Research*, 2(1), 20–31. [https://doi.org/10.26656/fr.2017.2\(1\).106](https://doi.org/10.26656/fr.2017.2(1).106)
41. Samard, S., Gu, B. Y., & Ryu, G. H. (2019). Effects of extrusion types, screw speed and addition of wheat gluten on physicochemical characteristics and cooking stability of meat analogues. *Journal of the Science of Food and Agriculture*, 99(11), 4922–4931. <https://doi.org/10.1002/jsfa.9722>
42. Lei, S., Zhao, C., Miao, Y., Zhao, H., Liu, Z., Zhang, Y., Zhao, L., Peng, C., & Gong, J. (2025). Quality characteristics and fibrous structure formation mechanism of walnut protein and wheat gluten meat analogues during high-moisture extrusion cooking process. *Food Chemistry*, 463(P2), 141168. <https://doi.org/10.1016/j.foodchem.2024.141168>
43. Schmid, E. M., Farahnaky, A., Adhikari, B., & Torley, P. J. (2022). High moisture extrusion cooking of meat analogs: A review of mechanisms of protein texturization. *Comprehensive Reviews in Food Science and Food Safety*, 21(6), 4573–4609. <https://doi.org/10.1111/1541-4337.13030>
44. Wang, Y., Xu, X., Feng, Y., Lv, F., Zhang, D., Ma, C., Li, H., & Wang, C. (2025). Modification mechanism of potato protein by twin-screw extrusion from the perspective of temperature variation. *Food Chemistry*, 472(August 2024), 142897. <https://doi.org/10.1016/j.foodchem.2025.142897>
45. Zhang, Y., & Ryu, G. H. (2023). Effects of process variables on the physicochemical, textural, and structural properties of an isolated pea protein-based high-moisture meat analog. *Foods*, 12(24), 4413. <https://doi.org/10.3390/foods12244413>
46. Maurya, A. K., & Said, P. P. (2014). Extrusion processing on physical and chemical properties of protein-rich products—An overview. *Journal of Bioresource Engineering and Technology*, 2(4), 61–67.
47. Agathian, G., Semwal, A. D., & Sharma, G. K. (2015). Optimization of barrel temperature and kidney bean flour percentage based on various physical properties of extruded snacks. *Journal of Food Science and Technology*, 52(7), 4113–4123. <https://doi.org/10.1007/s13197-014-1483-7>
48. Wu, M., Sun, Y., Bi, C., Ji, F., Li, B., & Xing, J. (2018). Effects of extrusion conditions on the physicochemical properties of soy protein/gluten composite. *International Journal of Agricultural and Biological Engineering*, 11(4), 205–210. <https://doi.org/10.25165/j.ijabe.20181104.4162>
49. Enobong, O. U., & Madu, O. I. (2023). Influence of extrusion process conditions on bulk density, water absorption capacity and oil absorption capacity of extruded aerial yam-soybean flour mixture. *African Journal of Food Science*, 17(6), 111–121. <https://doi.org/10.5897/ajfs2022.2180>
50. Kamani, M. H., Luithui, Y., & Meera, M. S. (2021). Upgrading black gram by-product to a new texturized vegetable source by extrusion: Evaluation of functionality, antinutrients and *in vitro* digestibility. *Waste and Biomass Valorization*, 12(8), 4319–4330. <https://doi.org/10.1007/s12649-020-01296-8>
51. Osen, R., Toelstede, S., Eisner, P., & Schweiggert-Weisz, U. (2015). Effect of high moisture extrusion cooking on protein-protein interactions of pea (*Pisum sativum* L.) protein isolates. *International Journal of Food Science and Technology*, 50(6), 1390–1396. <https://doi.org/10.1111/ijfs.12783>
52. Samard, S., & Ryu, G. H. (2019). Physicochemical and functional characteristics of plant protein-based meat analogs. *Journal of Food Processing and Preservation*, 43(10), Article e14123. <https://doi.org/10.1111/jfpp.14123>
53. Kyriakopoulou, K., Keppler, J. K., & van der Goot, A. J. (2021). Functionality of ingredients and additives in plant-based meat analogues. *Foods*, 10(3), Article 600. <https://doi.org/10.3390/foods10030600>
54. Daba, S. D., & Morris, C. F. (2022). Pea proteins: Variation, composition, genetics, and functional properties. *Cereal Chemistry*, 99(1), 8–20. <https://doi.org/10.1002/CCHE.10439>
55. Xiao, R., Flory, J., Alavi, S., & Li, Y. (2025). Physicochemical and functional properties of plant proteins before and after extrusion texturization. *Food Hydrocolloids*, 163(September 2024), 111119. <https://doi.org/10.1016/j.foodhyd.2025.111119>

56. Zhang, T., Yu, S., Pan, Y., Li, H., Liu, X., & Cao, J. (2023). Properties of texturized protein and performance of different protein sources in the extrusion process: A review. *Food Research International*, *174*, Article 113588. <https://doi.org/10.1016/j.foodres.2023.113588>
57. Ngounou Wetie, A. G., Sokolowska, I., Woods, A. G., Roy, U., Deinhardt, K., & Darie, C. C. (2014). Protein-protein interactions: Switch from classical methods to proteomics and bioinformatics-based approaches. *Cellular and Molecular Life Sciences*, *71*(2), 205–228. <https://doi.org/10.1007/s00018-013-1333-1>
58. Beck, S. M., Knoerzer, K., & Arcot, J. (2017). Effect of low moisture extrusion on a pea protein isolate's expansion, solubility, molecular weight distribution and secondary structure as determined by Fourier transform infrared spectroscopy (FTIR). *Journal of Food Engineering*, *214*, 166–174. <https://doi.org/10.1016/j.jfoodeng.2017.06.037>
59. Moreno, H. M., Tovar, C. A., Domínguez-Timón, F., Cano-Báez, J., Díaz, M. T., Pedrosa, M. M., & Borderías, A. J. (2020). Gelation of commercial pea protein isolate: Effect of microbial transglutaminase and thermal processing. *Food Science and Technology (Brazil)*, *40*(4), 800–809. <https://doi.org/10.1590/fst.19519>
60. Ketnawa, S., & Rawdkuen, S. (2023). Properties of texturized vegetable proteins from edible mushrooms by using single-screw extruder. *Foods*, *12*(6), Article 1269. <https://doi.org/10.3390/foods12061269>
61. Meng, X. Y., Zhu, X. Q., An, H. Z., Yang, J. F., & Dai, H. H. (2023). Study on the relationship between raw material characteristics of soybean protein concentrate and textured vegetable protein quality. *Food Science and Technology (Brazil)*, *43*, 1–10. <https://doi.org/10.1590/fst.121822>
62. Zhang, B., Kang, X., Cheng, Y., Cui, B., & Abd El-Aty, A. M. (2022). Impact of high moisture contents on the structure and functional properties of pea protein isolate during extrusion. *Food Hydrocolloids*, *127*, 107508. <https://doi.org/10.1016/j.foodhyd.2022.107508>
63. Singh, R., & Koksel, F. (2021). Effects of particle size distribution and processing conditions on the techno-functional properties of extruded soybean meal. *LWT*, *152*, 112321. <https://doi.org/10.1016/j.lwt.2021.112321>
64. Téllez-Morales, J. A., Herman-Lara, E., Gómez-Aldapa, C. A., & Rodríguez-Miranda, J. (2020). Techno-functional properties of the starch-protein interaction during extrusion-cooking of a model system (corn starch and whey protein isolate). *LWT*, *132*, 109789. <https://doi.org/10.1016/j.lwt.2020.109789>
65. Zhang, Y., Zhang, J., Chen, Q., He, N., & Wang, Q. (2022). High-moisture extrusion of mixed proteins from soy and surimi: Effect of protein gelling properties on the product quality. *Foods*, *11*(10), Article 1397. <https://doi.org/10.3390/foods11101397>